$B_{(s)} \to D_{(s)}^{(*)} M$ decays in the presence of final-state interactions

Albertus Hariwangsa Panuluh,[1,2,*] Satoshi Tanaka,[3,†] and Hiroyuki Umeeda[4,5,6,‡]

[1]*Department of Physics Education, Faculty of Teacher Training and Education, Sanata Dharma University, Paingan, Maguwohardjo, Sleman, Yogyakarta 55282, Indonesia*

[2]*Physics Program, Graduate School of Advanced Science and Engineering, Hiroshima University, 1-3-1 Kagamiyama, Higashi-Hiroshima 739-8526, Japan*

[3]*Scientific Computational Division, Nippon Advanced Information Service (NAIS Co., Inc.), 416 Muramatsu, Tokaimura, Naka-gun, Ibaraki 319-1112, Japan*

[4]*Center for Theoretical Physics and College of Physics, Jilin University, Changchun, 130012, China*

[5]*China Center of Advanced Science and Technology, Beijing 100190, China*

[6]*Institute of High Energy Physics, Chinese Academy of Sciences, Beijing 100049, China*

(Received 24 March 2025; accepted 22 April 2025; published 15 May 2025)

In light of the recent data for $\bar{B}_{(s)} \to D_{(s)}^{(*)} P$ and $\bar{B}_{(s)} \to D_{(s)} V$ decays, we perform a model-independent phenomenological analysis in the presence of quasielastic rescattering. With the Wilson coefficients including contributions beyond the standard model, the lifetimes of the B meson and $B_d^0 - \bar{B}_d^0$ mixing are investigated to clarify correlations among the observables. We show that parameter regions for quasielastic rescattering, the size of color-suppressed tree amplitudes, and new physics are constrained due to the lifetime data. As a consequence, it is revealed that this scenario can be tested by the future LHCb measurement of the width difference in $B_d^0 - \bar{B}_d^0$ mixing and semileptonic CP asymmetry.

DOI: 10.1103/PhysRevD.111.095020

I. INTRODUCTION

Decays of B mesons played an important role in testing the standard model (SM), as well as possible new physics (NP) contributions. Of the specific decay modes, nonleptonic channels are rather challenging processes in the context of strong interactions. A theoretical framework for these decays can be given by the QCD factorization (QCDF) approach [1]. In particular, it has been shown that for decays into heavy-light final states, such as $\bar{B}_d \to D^+ \pi^-$, vertex corrections are dominated by hard gluon exchange for large m_b (see Ref. [2] for the factorization proof in the soft-collinear effective theory). Furthermore, there exist no penguin or annihilation diagrams for the mentioned channel. Owing to this observation, $\bar{B}_d \to D^+ \pi^-$ decay is theoretically more tractable than those for light-light final states.

Recently, it was pointed out [3] that there are discrepancies between the experimental data[1] [6] and the prediction of the QCDF approach, where the theoretical analysis is performed at next-to-next-to-leading order (NNLO) [7]. It was also found that subleading power corrections, such as that from the three-particle Fock state of the light meson, etc., are not large enough to explain the data.[2] The mentioned circumstance possibly implies that final-state interactions (FSIs) [9,10] are required for the nonleptonic decays and/or NP contributions are present.

In previous works, FSIs were discussed in the Regge theory [11] and addressed in the QCDF approach [1]. A phenomenological framework incorporating FSIs was given by the quasielastic rescattering discussed in Refs. [12–15]: in the limit of SU(3) symmetry, where

*Contact author: panuluh@usd.ac.id
†Contact author: tanaka.satoshi.college@gmail.com
‡Contact author: umeeda@jlu.edu.cn

[1]See Ref. [4] for the recent experimental result. As to the theoretical side, recent discussion for $B \to DP$ decays in regards to SU(3) breaking was found in Ref. [5].

[2]In another recent work [8], the analysis was carried out in light-cone QCD sum rules, giving an alternative prediction to the QCDF. While explaining the data within uncertainty, it was commented [8] that the additional investigations are required in view of the limited precision in the nonperturbative input.

mesons in the same flavor multiplet degenerate, FSIs are given by a mixing matrix that acts on the amplitudes with specific final states. An observable effect is a change in the relative phase between the amplitudes with final states lying in different SU(3) multiplets, since mixing between states with different quantum numbers does not occur and thus it only alters the phases. Formulated in this way, the quasielastic rescattering gives a tractable approach for including two-body FSIs.

In Ref. [16], it was shown that, even if the quasielastic rescattering is incorporated, the puzzle for the branching ratios cannot be resolved in a reasonable way, in the sense that color-allowed and color-suppressed processes are not simultaneously explained, with an overall coefficient of the color-suppressed tree amplitude treated as a free parameter. In this circumstance, the possibility that NP is affecting the short-distance Wilson coefficients is not straightforwardly ruled out and was investigated [16] with the FSIs, where parameter regions are more extended as compared to the case without rescattering. See Refs. [17–20] for further studies in the context beyond the SM.

It is worth noting that the aforementioned scenario with NP is supposed to confront constraints from other observables with nonleptonic transitions. This was pointed out in Ref. [3] (see also Ref. [21]), while dedicated numerical results were obtained in Ref. [22]. In particular, the total widths of the B meson and $B_d^0 - \bar{B}_d^0$ mixing (see Refs. [23,24] for recent analyses) are considered as constraints on the NP scenario. For the former, a lifetime ratio $\tau(B^+)/\tau(B_d)$ plays a particularly suitable role, since theoretical uncertainty is better controlled and is characterized by the contribution of Pauli interference.

In this work, we carry out a phenomenological analysis of $B_{(s)} \to D_{(s)}^{(*)} M$ in the presence of the quasielastic rescattering and clarify its correlation with $\tau(B^+)/\tau(B_d)$ and $B_d^0 - \bar{B}_d^0$ mixing. We show that these observables lead to constraints and/or predictions of the scenario in which rescattering contributions are involved in $B_{(s)} \to D_{(s)}^{(*)} M$ decays. In particular, it is demonstrated that some of the model-parameter space is significantly constrained to explain the observables. As a resulting prediction, the width difference $(\Delta\Gamma_d)$ and the semileptonic CP asymmetry $(\mathcal{A}_{\rm SL}^d)$ are evaluated.

This paper is organized as follows. In Sec. II, a basic framework for quasielastic rescattering is introduced for $B \to DM$ decays. The constraints from branching ratios on the model parameters are obtained in an analytical manner for both $b \to c\bar{u}s$ and $b \to c\bar{u}d$ transitions. The SU(3) symmetry breaking is considered within the formalism for the latter processes. In Secs. III and IV, B-meson lifetimes and $B^0 - \bar{B}^0$ mixing are respectively discussed. In Sec. V, the phenomenological analysis is given for the mentioned observables. The correlation patterns for QCD factorization parameters and the rescattering angle satisfying the phenomenological constraints are obtained numerically. We show that this scenario can be testable via $\Delta\Gamma_d$ and $\mathcal{A}_{\rm SL}^d$ with future LHCb measurements. Finally, concluding remarks are given in Sec. VI.

II. $B \to DM$ DECAYS

In this section, we investigate B-meson nonleptonic decays into two-body exclusive final states that include a charmed meson. The effective Hamiltonian relevant for $b \to c\bar{q}_2 q_3$ $(q_2 = u, c, q_3 = d, s)$ is given by

$$\mathcal{H}_W = \frac{G_F}{\sqrt{2}}\left[V_{cb}V_{q_2q_3}^* \sum_{i=1}^{2} c_i Q_i^{\bar{q}_2 q_3} - V_{tb}V_{tq_3}^*\left(\sum_{i=3}^{6} c_i Q_i^{q_3} + c_8 Q_8^{q_3}\right)\right]. \quad (2.1)$$

The definitions of the operators that appear in Eq. (2.1) are given in Appendix B 1. The radiative QCD corrections to the Wilson coefficient can be obtained in Ref. [25] and references therein, with a certain care of the difference in the notation.

A. Quasielastic rescattering

Here we recapitulate the FSI discussed in Refs. [12–15]; see also Ref. [16]. Decay amplitudes without FSIs are given by vector notations and classified as A_{S,I_z}, where S and I_z denote the strangeness and the diagonalized component of isospin,

$$\mathcal{A}_{-1,0} = \begin{pmatrix} \mathcal{A}(\bar{B}^0 \to D^+K^-) \\ \mathcal{A}(\bar{B}^0 \to D^0\bar{K}^0) \end{pmatrix},$$
$$\mathcal{A}_{1,-1} = \begin{pmatrix} \mathcal{A}(\bar{B}_s^0 \to D_s^+\pi^-) \\ \mathcal{A}(\bar{B}_s^0 \to D^0K^0) \end{pmatrix}. \quad (2.2)$$

The FSIs can be taken into account by the quasielastic scattering; due to $\bar{3} \times 8 = \overline{15} + 6 + \bar{3}$ for the final state that consists of $D\Pi$, where Π is an SU(3) octet state, the rescattering matrix is decomposed as [12–14]

$$S^{1/2} = e^{i\delta_{\overline{15}}}|\overline{15}; a\rangle\langle\overline{15}; a| + e^{i\delta_6}|6; b\rangle\langle 6; b| + \sum_{m,n=\bar{3},\bar{3}'} |m; c\rangle\mathcal{U}_{mn}^{1/2}\langle n; c|. \quad (2.3)$$

For the $\overline{15}$ and 6 terms in Eq. (2.3), in the limit of the flavor symmetry, the final states with definitive quantum numbers such as isospin do not mix under the FSIs and thus the rescattering merely alters the phase of the amplitude. In contrast to this case, for the last term in Eq. (2.3), one needs to take account of the mixing between $\bar{3}$ and $\bar{3}'$ states in the presence of the SU(3) singlet state that consists of light flavors accompanied by a D meson. This is represented as 2×2 matrix given by $\mathcal{U}_{mn}^{1/2}$ in Eq. (2.3).

Incorporating the FSIs, the amplitudes in Eq. (2.2) are modified as

$$\mathcal{A}^f_{S,I_z} = V^{-1}_{S,I_z} S^{1/2}_{S,I_z} V_{S,I_z} \mathcal{A}_{S,I_z}, \tag{2.4}$$

where $S^{1/2}_{S,I_z}$ represents the rescattering matrix for specific quantum numbers, while V_{S,I_z} is a diagonal matrix defined by [15,16]

$$V_{-1,0} = \mathrm{diag}(1,1), \qquad V_{1,-1} = \mathrm{diag}\left(1, \frac{f_{D_s} f_\pi}{f_D f_K}\right). \tag{2.5}$$

Due to Eq. (2.5), SU(3) breaking for the rescattering is included in $b \to c\bar{u}d$ via the decay constants, but not in $b \to c\bar{u}s$. If we consider the state with $S = -1$ and $I_z = 0$ as an example, the rescattering matrix that mixes D^+K^- and $D^0\bar{K}^0$ final states can be obtained from components of the SU(3) representations,

$$\overline{15}(S=-1, I=1): \ \frac{1}{\sqrt{2}}(|D^+K^-\rangle + |D^0\bar{K}^0\rangle), \tag{2.6}$$

$$6(S=-1,\ I=0): \ \frac{1}{\sqrt{2}}(|D^+K^-\rangle - |D^0\bar{K}^0\rangle), \tag{2.7}$$

without antitriplet states. Likewise, the decomposition of $S = 1$, $I_z = -1$ can also be obtained. The above relations are readily solved with respect to $|D^+K^-\rangle$ and $|D^0\bar{K}^0\rangle$. By acting the matrix in Eq. (2.3) on those states for both $S = -1$, $I_z = 0$ and $S = 1$, $I_z = -1$, one can obtain [12]

$$S^{1/2}_{-1,0} = S^{1/2}_{1,-1} = \frac{e^{i\delta_{\overline{15}}}}{2}\begin{pmatrix} 1+e^{i\delta'} & 1-e^{i\delta'} \\ 1-e^{i\delta'} & 1+e^{i\delta'} \end{pmatrix}, \quad \delta' = \delta_6 - \delta_{\overline{15}}, \tag{2.8}$$

where the overall phase denoted by $\delta_{\overline{15}}$ cancels out when the branching ratios are calculated. It should be noted that for the above two choices of strangeness and isospin, the antitriplet term in Eq. (2.3) is not involved in the discussion.

In the following sections, we also discuss processes with final states of $S = 0$, $I_z = 3/2$ and $S = 1$, $I_z = 1$, corresponding, e.g., to $B^+ \to \bar{D}^0\pi^+$ and $B^+ \to \bar{D}^0 K^+$. These cases do not undergo the rescattering since there are no other decay channels that mix together. Hence, the rescattering is considered for the $S = -1$, $I_z = 0$ and $S = 1$, $I_z = -1$ cases (or their CP-conjugate processes) individually.

B. Branching ratios

In this section, relations constraining parameters of the QCDF approach and rescattering from branching ratios of B-meson two-body decays are obtained. For definitiveness, the discussion of $\bar{B} \to D\bar{K}$, which proceeds via $b \to c\bar{u}s$, is given first. Subsequently, other processes with $b \to c\bar{u}d$ transitions are also analyzed. The resulting relations in Eqs. (2.16)–(2.18) and (2.29)–(2.31) play a major role in the numerical analysis.

1. $b \to c\bar{u}s$

Below, $\bar{B} \to D\bar{K}$ with the final state that consists of two pseudoscalars is discussed first. In the presence of the rescattering, branching ratios of the nonleptonic decays are

$$\mathrm{Br}^{ij} \equiv \mathrm{Br}[P \to M_1^i M_2^j] = \frac{\tau^{ij} p_{\mathrm{cm}}[P \to M_1^i M_2^j]}{8\pi m_P^2} |V_{cb}V^*_{us}|^2 |\mathcal{A}_f[P \to M_1^i M_2^j]|^2, \tag{2.9}$$

with $(i,j) = (+,-), (0,0), (0,-)$, and τ^{ij} denoting a lifetime of the initial particle, which is $\tau(B^+), \tau(B_d)$, or $\tau(B_s)$. In Eq. (2.9), p_{cm} is a momentum of either particle in the final state defined in the rest frame of the initial particle,

$$p_{\mathrm{cm}}[P \to M_1 M_2] = \frac{1}{2m_P}\sqrt{[m_P^2 - (m_{M_1} + m_{M_2})^2][m_P^2 - (m_{M_1} - m_{M_2})^2]}. \tag{2.10}$$

In Eq. (2.9), the subscript f represents the presence of FSIs.

In the case without rescattering, the processes are represented by topological amplitudes,

$$\mathcal{A}^{+-} \equiv \mathcal{A}[\bar{B}^0 \to D^+K^-] = T_{DK}, \tag{2.11}$$

$$\mathcal{A}^{00} \equiv \mathcal{A}[\bar{B}^0 \to D^0\bar{K}^0] = C_{DK}, \tag{2.12}$$

$$\mathcal{A}^{0-} \equiv \mathcal{A}[B^- \to D^0K^-] = T_{DK} + C_{DK}, \tag{2.13}$$

where T_{DK} and C_{DK} are color-allowed and -suppressed tree diagrams, respectively. In the QCDF approach [1], these amplitudes are evaluated as

$$T_{DK} = N^T_{DK} a_1, \qquad C_{DK} = N^C_{DK} a_2^{\mathrm{eff}}. \tag{2.14}$$

In the above relation, $N^{T(C)}_{DK}$ is a normalization factor that is a product of the Fermi constant, the decay constant, and the form factor defined in Eq. (A1). For later convenience, we introduce the notation

$$\bar{a}_2 = (N^C_{DK} a_2^{\rm eff})/(N^T_{DK} a_1). \tag{2.15}$$

By using the three relations for $(i,j) = (+,-), (0,0)$, and $(0,-)$ in Eq. (2.9), one can determine $\mathrm{Re}(\bar{a}_2), \mathrm{Im}(\bar{a}_2)$, and δ' with the branching ratio data and a given value of a_1. With the derivation discussed in Appendix A 1, the results read

$$\mathrm{Re}(\bar{a}_2) = \frac{(\tau^{+-}/\tau^{0-})\mathrm{Br}^{0-} - \mathrm{Br}^{+-} - \mathrm{Br}^{00}}{2\mathcal{N}_{DK}}, \tag{2.16}$$

$$\mathrm{Im}(\bar{a}_2) = \pm\sqrt{\frac{\mathrm{Br}^{+-} + \mathrm{Br}^{00}}{\mathcal{N}_{DK}} - 1 - [\mathrm{Re}(\bar{a}_2)]^2}, \tag{2.17}$$

$$\delta' = \mathrm{Arcsin}\left[\frac{\mathrm{Br}^{+-} - \mathrm{Br}^{00}}{\mathcal{N}_{DK}\sqrt{A^2_{DK} + B^2_{DK}}}\right] - \omega_{DK}, \times \pi - \mathrm{Arcsin}\left[\frac{\mathrm{Br}^{+-} - \mathrm{Br}^{00}}{\mathcal{N}_{DK}\sqrt{\bar{A}^2_{DK} + \bar{B}^2_{DK}}}\right] - \omega_{DK} \pmod{2\pi}, \tag{2.18}$$

where the definitions of $\mathcal{N}_{DK}, A_{DK}, B_{DK}$, and ω_{DK} are given in Appendix A 1. It should be noted that there are twofold ambiguities for δ' and the sign of $\mathrm{Im}(\bar{a}_2)$. The solutions in Eqs. (2.16)–(2.18) exist only if the following conditions are satisfied:

$$\mathcal{N}_{DK} \neq 0, \tag{2.19}$$

$$\frac{\mathrm{Br}^{+-} + \mathrm{Br}^{00}}{\mathcal{N}_{DK}} - [\mathrm{Re}(\bar{a}_2)]^2 \geq 1, \tag{2.20}$$

$$-1 \leq \frac{\mathrm{Br}^{+-} - \mathrm{Br}^{00}}{\mathcal{N}_{DK}\sqrt{A^2_{DK} + B^2_{DK}}} \leq 1. \tag{2.21}$$

The above conditions follow from the derivation procedure in Appendix A 1.

In what follows, the cases of $\bar{B} \to D\bar{K}^*$ and $\bar{B} \to D^*\bar{K}$ decays are discussed to obtain relations similar to Eqs. (2.16)–(2.21). For processes including a vector meson in the final state, a formula for branching ratios analogous to Eq. (2.9) is

$$\mathrm{Br}[P \to M_1^* M_2] = \frac{\tau_P p_{\rm cm}[P \to M_1^* M_2]}{8\pi m_P^2} |V_{cb}V_{us}^*|^2 \sum_\epsilon |\mathcal{A}_f[P \to M_1^* M_2]|^2, \tag{2.22}$$

$$\mathrm{Br}[P \to M_1 M_2^*] = \frac{\tau_P p_{\rm cm}[P \to M_1 M_2^*]}{8\pi m_P^2} |V_{cb}V_{us}^*|^2 \sum_\epsilon |\mathcal{A}_f[P \to M_1 M_2^*]|^2. \tag{2.23}$$

For the amplitudes in Eqs. (2.22) and (2.23), the polarization is factored out as follows:

$$\mathcal{A}_f[P \to M_1^* M_2] = (\epsilon^* \cdot p_B)\bar{\mathcal{A}}_f[P \to M_1^* M_2], \quad \mathcal{A}_f[P \to M_1 M_2^*] = (\epsilon^* \cdot p_B)\bar{\mathcal{A}}_f[P \to M_1 M_2^*]. \tag{2.24}$$

By evaluating the polarization sum,

$$\sum_\epsilon |\epsilon^* \cdot p_B|^2 = \left(\frac{m_B}{m_V} p_{\rm cm}\right)^2, \tag{2.25}$$

the branching ratios in Eqs. (2.22) and (2.23) are recast into the forms

$$\mathrm{Br}[P \to M_1^* M_2] = \frac{\tau_P p^3_{\rm cm}[P \to M_1^* M_2]}{8\pi m^2_{M_1^*}} |V_{cb}V_{us}^*|^2 |\bar{\mathcal{A}}_f[P \to M_1^* M_2]|^2, \tag{2.26}$$

$$\mathrm{Br}[P \to M_1 M_2^*] = \frac{\tau_P p^3_{\rm cm}[P \to M_1 M_2^*]}{8\pi m^2_{M_2^*}} |V_{cb}V_{us}^*|^2 |\bar{\mathcal{A}}_f[P \to M_1 M_2^*]|^2. \tag{2.27}$$

One can also obtain the resulting relations in Eqs. (2.16)–(2.21) for $\bar{B} \to D\bar{K}^*$ and $\bar{B} \to D^*\bar{K}$ by simply replacing $D \to D^*$ and $K \to K^*$, respectively, with the proper replacement of data for the branching ratio on the rhs. The definitions of normalization factors for the case including a vector meson are given in Eqs. (A2) and (A3).

2. $b \to c\bar{u}d$

By making some replacements in the previous discussions for $b \to c\bar{u}s$ decays, we can also obtain similar results for $b \to c\bar{u}d$ decays. In this case, nonvanishing SU(3) breaking for the rescattering in Eq. (2.5) must be taken into account. In addition, mass differences in hadrons for

normalization factors and phase space need to be consistently included, unlike the case of $b \to c\bar{u}s$ decays, where the isospin symmetry relates the masses of the relevant particles. The parameters relevant for SU(3) breaking are defined in Appendix A 2.

For $b \to c\bar{u}d$, we introduce a normalized coefficient for color-suppressed tree diagram,

$$\bar{a}_2 = (N_C^{D^0\bar{K}^0} a_2^{\rm eff})/(N_T^{D_s^+\pi^-} a_1). \tag{2.28}$$

The above object is not to be confused with the one for $b \to c\bar{u}s$ in Eq. (2.15).

In a way analogous to $b \to c\bar{u}s$ decays, solutions of the parameters for $b \to c\bar{u}d$ decays are

$$\mathrm{Re}(\bar{a}_2) = \frac{(1+\Delta^{(1)}_{DP})\frac{\tau^{+-}}{\tau^{0-}}\mathrm{Br}^{0-} - (1+\Delta^{(2)}_{DP})[\mathrm{Br}^{+-} + (1+\Delta^{(3)}_{DP})\mathrm{Br}^{00}]}{2\mathcal{N}_{D_s^+\pi^-}} - \frac{1}{2}(1+\Delta^{(2)}_{DP})\Delta^{(4)}_{DP}, \tag{2.29}$$

$$\mathrm{Im}(\bar{a}_2) = \pm\sqrt{(1+\Delta^{(5)}_{DP})\left[\frac{\mathrm{Br}^{+-} + (1+\Delta^{(3)}_{DP})\mathrm{Br}^{00}}{\mathcal{N}_{D_s^+\pi^-}} - 1\right] - [\mathrm{Re}(\bar{a}_2)]^2}, \tag{2.30}$$

$$\begin{aligned}\delta' = &\mathrm{Arcsin}\left(\frac{\mathrm{Br}^{+-} - (1+\Delta^{(3)}_{DP})\mathrm{Br}^{00}}{\mathcal{N}_{D_s^+\pi^-}\sqrt{A_{DP}^2 + B_{DP}^2}}\right) - \omega_{DP}, \\ &\times\pi - \mathrm{Arcsin}\left(\frac{\mathrm{Br}^{+-} - (1+\Delta^{(3)}_{DP})\mathrm{Br}^{00}}{\mathcal{N}_{D_s^+\pi^-}\sqrt{A_{DP}^2 + B_{DP}^2}}\right) - \omega_{DP} \pmod{2\pi},\end{aligned} \tag{2.31}$$

where the definitions of $\Delta^{(i)}_{DP}(i = 1, \ldots, 5)$, $\mathcal{N}_{D_s^+\pi^-}$, ω_{DP}, A_{DP}, and B_{DP} are given in Appendix A 2. It is found that the twofold ambiguities exist for Eqs. (2.30) and (2.31) and $b \to c\bar{u}s$ decays. The solutions in Eqs. (2.29)–(2.31) exist only if the conditions given below are satisfied:

$$\mathcal{N}_{D_s^+\pi^-} \neq 0, \tag{2.32}$$

$$(1+\Delta^{(5)}_{DP})\left[\frac{\mathrm{Br}^{+-} + (1+\Delta^{(3)}_{DP})\mathrm{Br}^{00}}{\mathcal{N}_{D_s^+\pi^-}} - 1\right] - [\mathrm{Re}(\bar{a}_2)]^2 \geq 0, \tag{2.33}$$

$$-1 \leq \frac{\mathrm{Br}^{+-} - (1+\Delta^{(3)}_{DP})\mathrm{Br}^{00}}{\mathcal{N}_{D_s^+\pi^-}\sqrt{A_{DP}^2 + B_{DP}^2}} \leq 1. \tag{2.34}$$

As shown in Eqs. (A19) and (A20), $\Delta^{(i)}_{DP}$ vanishes in the SU(3) limit. Hence, the structures of Eqs. (2.29)–(2.34) for $b \to c\bar{u}d$ are reduced to those for $b \to c\bar{u}s$ in Eqs. (2.16)–(2.21) in the SU(3) limit. It should be noted that the dependence on heavy-to-light form factors appears solely from $\Delta^{(2)}_{DP}$ in Eq. (A19).

For other $b \to c\bar{u}d$ decays including a vector meson, the result corresponding to $\bar{B} \to D^* P$ can be obtained by the replacement of $D \to D^*$, while the one for $\bar{B} \to DV$ decay can be given by $P \to V$, $K \to K^*$, and $\pi \to \rho$ in Eqs. (2.29)–(2.34).

III. LIFETIMES OF B MESONS

In this section, we recapitulate how the total width of beauty mesons is evaluated at leading order (LO) in QCD. This observable is analyzed by means of the heavy quark expansion (HQE): after the correlation functions are computed in the Euclidean domain, the expression is analytically continued to the Minkowski region, leading to the $1/m_b$ expansion for the observable. See Refs. [23,26] for the recent works within the SM.

We restrict ourselves to the isospin limit, where μ_π, μ_G for B_d are identical to those for B^+. With $q = u, d$ and $B_u = B^+$, the total width is written as

$$\Gamma(B_q) = \Gamma^{\text{2-quark}} + \Gamma_q^{\text{4-quark}}. \tag{3.1}$$

The lifetime ratio is calculated from the above objects,

$$\frac{\tau(B^+)}{\tau(B_d)} = 1 - \frac{\Gamma(B^+) - \Gamma(B_d)}{\Gamma(B^+)} = 1 - \frac{\Gamma_u^{\text{4-quark}} - \Gamma_d^{\text{4-quark}}}{\Gamma(B^+)}. \tag{3.2}$$

In the isospin limit for the matrix elements, $\tau(B^+)/\tau(B_d) - 1$ is proportional to the spectator effect. In what follows, the two terms in Eq. (3.1) are discussed.

A. Two-quark operators

In the limit of the isospin symmetry, $\Gamma^{\text{2-quark}}$ in Eq. (3.1) does not depend on the label of q. The contributions from two-quark operators in the above equation are classified by the nonleptonic and semileptonic pieces,

$$\Gamma^{\text{2-quark}} = \sum_{q_2, q_3} \Gamma_{\rm NL}(b \to c\bar{q}_2 q_3) + \sum_{\ell} \Gamma_{\rm SL}(b \to c\ell\bar{\nu}), \tag{3.3}$$

where the summations are taken for all of the possible combinations with $q_2 = u, c$, $q_3 = d, s$, and $\ell = e, \mu, \tau$. It should be noted that the $b \to u$ transition, neglected in

Eq. (3.3), is Cabibbo suppressed, while larger contributions arise from $b \to c$. The partial widths that appear in Eq. (3.3) are expanded by $1/m_b$, leading to

$$\Gamma_{\rm NL}(b \to c\bar{q}_2 q_3) = \Gamma_0 |V_{cb} V^*_{q_2 q_3}|^2 \times \left(C_{\rm LP}^{c\bar{q}_2 q_3} + C_\pi^{c\bar{q}_2 q_3} \frac{\mu_\pi^2}{m_b^2} + C_G^{c\bar{q}_2 q_3} \frac{\mu_G^2}{m_b^2} \right), \tag{3.4}$$

$$\Gamma_{\rm SL}(b \to c\ell\bar{\nu}) = \Gamma_0 |V_{cb}|^2 \left(C_{\rm LP}^{c\ell\bar{\nu}} + C_\pi^{c\ell\bar{\nu}} \frac{\mu_\pi^2}{m_b^2} + C_G^{c\ell\bar{\nu}} \frac{\mu_G^2}{m_b^2} \right), \tag{3.5}$$

where $\Gamma_0 = G_F^2 m_b^5/(192\pi^3)$. The matrix elements of the two-quark operators, μ_π^2 and μ_G^2, are defined in Eq. (B10). Furthermore, the nonleptonic coefficients in Eq. (3.4) stem from quadratic combinations of the $|\Delta B| = 1$ Wilson coefficients,

$$C_I^{c\bar{q}_2 q_3} = 3c_1^2 \mathcal{C}_{I,11}^{c\bar{q}_2 q_3} + 2c_1 c_2 \mathcal{C}_{I,12}^{c\bar{q}_2 q_3} + 3c_2^2 \mathcal{C}_{I,22}^{c\bar{q}_2 q_3}, \tag{3.6}$$

where $I = {\rm LP}, \pi, G$. In Eq. (3.6), the contribution of NP is contained only in c_1 and c_2, while $\mathcal{C}_{I,ij}^{c\bar{q}_2 q_3}(i,j = 1,2, I = {\rm LP}, \pi, G)$ can be obtained in previous works, e.g., Ref. [27] and references therein.

B. Four-quark operators

The contribution of the spectator effect in Eq. (3.1) is rewritten as

$$\Gamma_u^{\text{4-quark}} = \Gamma_{\rm int}, \qquad \Gamma_d^{\text{4-quark}} = \Gamma_{\rm ann}, \tag{3.7}$$

where int and ann represent the Pauli interference and weak annihilation, respectively. The above objects are proportional to the matrix elements of four-quark operators defined in Eqs. (B11)–(B18). In the case of dimension-six contributions, the matrix elements can be obtained from Ref. [28], while dimension-seven operators are evaluated via the vacuum insertion approximation, leading to [29]

$$\Gamma_{\rm int} = \frac{G_F^2 m_b^2}{12\pi} |V_{cb} V^*_{ud}|^2 f_B^2 m_B (1-z)^2 \left\{ (c_1^2 + c_2^2 + 6c_1 c_2) \times \left[B_1 - \left(\frac{1+z}{1-z} + \frac{1}{2} \right) \left(\frac{m_B^2}{m_b^2} - 1 \right) \right] + 6(c_1^2 + c_2^2)\epsilon_1 \right\}, \tag{3.8}$$

$$\Gamma_{\rm ann} = -\frac{G_F^2 m_b^2}{12\pi} |V_{cb} V^*_{ud}|^2 f_B^2 m_B (1-z)^2 \left\{ \left(\frac{c_1^2}{3} + 2c_1 c_2 + 3c_2^2 \right) \left[\left(1 + \frac{z}{2} \right) B_1 - (1+2z) B_2 + \left[\frac{1+z+z^2}{1-z} + \frac{6z^2}{1-z} - \frac{1}{2}\left(1+\frac{z}{2}\right) - \frac{1}{2}(1+2z) \right] \left(\frac{m_B^2}{m_b^2} - 1 \right) \right] + 2c_1^2 \left[\left(1 + \frac{z}{2} \right) \epsilon_1 - (1+2z)\epsilon_2 \right] \right\}. \tag{3.9}$$

In the above relations, z represents $(m_c/m_b)^2$.

IV. $B_d^0 - \bar{B}_d^0$ MIXING

In this section, observables for neutral meson mixing of beauty mesons are discussed. In previous works, NP contributions to the width differences in the $D^0 - \bar{D}^0$ and $B_s^0 - \bar{B}_s^0$ mixings were discussed in Refs. [30–32]. Moreover, CP violation in the $B^0 - \bar{B}^0$ mixing was also investigated beyond the SM in Refs. [32–40].

A. Dispersive part and absorptive part

The dispersive part for the $B_d^0 - \bar{B}_d^0$ mixing amplitude in the SM is dominated by the contribution of intermediate top quarks. In this case, an expression where external quark momenta and masses are neglected, represented by the Inami-Lim function [41],

$$M_{21} = \frac{G_F^2 M_W^2}{12\pi^2} m_{B_d} f_{B_d}^2 [\eta(\mu_b)]_{\rm VLL} B_1^d(\mu_b) S_0\left(\frac{\bar{m}_t^2(m_t)}{M_W^2} \right) \times (V_{tb}^* V_{td})^2, \tag{4.1}$$

$$S_0(x) = \frac{4x - 11x^2 + x^3}{4(1-x)^2} - \frac{3x^3 \ln x}{2(1-x)^3}, \tag{4.2}$$

gives an excellent approximation.

For the absorptive part, the theoretical analysis can be performed by HQE, analogously to the total width of B mesons. In contrast to the case of the total width, the leading contribution to the width difference arises from four-quark operators. At next-to-leading order (NLO) in power corrections $(1/m_b)$, the width difference in the $B^0 - \bar{B}^0$ mixing is obtained [42–44].[3] The SM contribution to Γ_{21} in the $B_d^0 - \bar{B}_d^0$ mixing with NLO power correction is given by [43]

$$\Gamma_{21} = -\frac{G_F^2 m_b^2}{24\pi m_{B_d}} [c_1^{d,\rm mix}(\mu_2) \langle \bar{B}_d^0 | \mathcal{O}_1^d | B_d^0 \rangle + c_2^{d,\rm mix}(\mu_2) \langle \bar{B}_d^0 | \mathcal{O}_2^d | B_d^0 \rangle + \delta_{1/m}^d]. \tag{4.3}$$

The expressions for the coefficients are given by [43]

[3] See also NNLO in the power correction $(1/m_b^2)$ in Ref. [32].

$$c_k^{d,\mathrm{mix}} = (V_{tb}^* V_{td})^2 D_k^{uu} + 2V_{cb}^* V_{cd} V_{tb}^* V_{td}(D_k^{uu} - D_k^{cu}) + (V_{cb}^* V_{cd})^2 (D_k^{uu} + D_k^{cc} - 2D_k^{cu}), \qquad (k = 1, 2) \tag{4.4}$$

$$\delta_{1/m}^d = (V_{tb}^* V_{td})^2 \delta_{1/m}^{uu\,d} + 2V_{cb}^* V_{cd} V_{tb}^* V_{td}(\delta_{1/m}^{uu\,d} - \delta_{1/m}^{cu\,d}) + (V_{cb}^* V_{cd})^2 (\delta_{1/m}^{uu\,d} + \delta_{1/m}^{cc\,d} - 2\delta_{1/m}^{cu\,d}). \tag{4.5}$$

For $(q_1, q_2) = (c, c), (c, u)$, and (u, u) with $k = 1, 2$,

$$D_k^{q_1 q_2}(\mu_2) = \sum_{i,j=1,2} c_i(\mu_1) c_j(\mu_1) F_{k,ij}^{q_1 q_2,\mathrm{mix}}(\mu_1, \mu_2) + \frac{\alpha_s}{4\pi} [c_1(\mu_1)]^2 P_{k,11}^{q_1 q_2}(\mu_1, \mu_2) + \frac{\alpha_s}{4\pi} c_1 c_8 (P_{k,18}^{q_1} + P_{k,18}^{q_2}) + \sum_{i=1,2} \sum_{r=3,6} c_i c_r (P_{k,ir}^{q_1} + P_{k,ir}^{q_2}). \tag{4.6}$$

The phase-space functions were calculated in Refs. [43,45] at the precision of NLO in QCD. It should be noted that in our notation of c_1 and c_2, we need to replace the indices $1 \to 2$ and $2 \to 1$ for i, j in Refs. [43,45]. The phase-space integral proportional to the quadratic term with respect to c_1 and c_2 is decomposed by the LO and NLO parts in QCD,

$$F_{k,ij}^{q_1 q_2,\mathrm{mix}} = A_{k,ij}^{q_1 q_2,\mathrm{mix}} + \frac{\alpha_s}{4\pi} B_{k,ij}^{q_1 q_2,\mathrm{mix}}. \tag{4.7}$$

$A_{k,ij}^{q_1 q_2,\mathrm{mix}}$ and $B_{k,ij}^{q_1 q_2,\mathrm{mix}}$ in Eq. (4.7), as well as the phase-space functions related to the penguin operators in Eq. (4.6), can be extracted from Ref. [43], while $D_k^{cu,\mathrm{mix}}$ can be extracted from Ref. [45].

The dimension-seven contributions were also obtained in Ref. [43],

$$\delta_{1/m}^{cc\,d} = \sqrt{1-4z}\Big\{(1+2z)[K_2(\langle R_2^d\rangle + 2\langle R_4^d\rangle) - 2K_1(\langle R_1^d\rangle + \langle R_2^d\rangle)] - \frac{12z^2}{1-4z}[K_1(\langle R_2^d\rangle + 2\langle R_3^d\rangle) + 2K_2\langle R_3^d\rangle]\Big\}, \tag{4.8}$$

$$\delta_{1/m}^{cu\,d} = (1-z)^2\Big\{(1+2z)[K_2(\langle R_2^d\rangle + 2\langle R_4^d\rangle) - 2K_1(\langle R_1^d\rangle + \langle R_2^d\rangle)] - \frac{6z^2}{1-z}[K_1(\langle R_2^d\rangle + 2\langle R_3^d\rangle) + 2K_2\langle R_3^d\rangle]\Big\}, \tag{4.9}$$

$$\delta_{1/m}^{uu\,d} = K_2(\langle R_2^d\rangle + 2\langle R_4^d\rangle) - 2K_1(\langle R_1^d\rangle + \langle R_2^d\rangle), \tag{4.10}$$

with $K_1 = 3c_2^2 + 2c_1 c_2$ and $K_2 = c_1^2$. The width difference in the B_d system is given by [43]

$$\Delta\Gamma_d = -2|M_{21}|\mathrm{Re}\left(\frac{\Gamma_{21}}{M_{21}}\right). \tag{4.11}$$

B. *CP* violation

CP violation in the $B_d^0 - \bar{B}_d^0$ mixing can be measured in, e.g., the semileptonic *CP* asymmetry, given by

$$\mathcal{A}_{\mathrm{SL}}^d(t) = \frac{N[\bar{B}_d^0(t) \to \ell^+ \nu_\ell X] - N[B_d(t) \to \ell^- \bar{\nu}_\ell X]}{N[\bar{B}_d^0(t) \to \ell^+ \nu_\ell X] + N[B_d(t) \to \ell^- \bar{\nu}_\ell X]}, \tag{4.12}$$

where the above object is approximated to an excellent precision as

$$\mathcal{A}_{\mathrm{SL}}^d = \frac{|p/q|^2 - |q/p|^2}{|p/q|^2 + |q/p|^2} \simeq \mathrm{Im}\left(\frac{\Gamma_{12}}{M_{12}}\right). \tag{4.13}$$

In Eq. (4.13), M_{12} and Γ_{12} are calculated as complex conjugate of Eqs. (4.1) and (4.3).

V. NUMERICAL RESULTS

In the analysis, $\mathrm{Re}(\bar{a}_2), \mathrm{Im}(\bar{a}_2)$, and δ' are treated as parameters determined in the numerical result, since they are not predictable within the QCDF approach. As to the color-allowed tree diagram, the coefficient consists of the SM part and NP contributions,

$$a_1(m_b) = a_1^{\mathrm{SM}}(m_b) + c_1^{\mathrm{NP}}(m_b) + \frac{c_2^{\mathrm{NP}}(m_b)}{3}. \tag{5.1}$$

For the SM contribution, the universal value of $a_1^{\mathrm{SM}}(m_b) = 1.070 \pm 0.012$ [16] is adopted, realized to the high precision [7] at NNLO. Contributions beyond the SM are included at the scale of $\mu = M_W$,

$$c_i(M_W) = c_i^{\mathrm{SM}}(M_W) + c_i^{\mathrm{NP}}(M_W) \quad (i = 1, 2), \tag{5.2}$$

while the Wilson coefficients of the (chromomagnetic) penguin operators are fixed to the SM values at the same scale. Here $c_i^{\mathrm{NP}}(M_W)$ $(i = 1, 2)$ in Eq. (5.2) is set to a real-valued parameter and is taken as independent of the flavors, which universally affect $b \to c\bar{q}_2 q_3$ for $q_2 = u$, c and $q_3 = d$, s. With Eq. (5.2), the radiative corrections are discussed separately for the SM and NP, where LO is sufficiently accurate for NP,

$$\begin{pmatrix} c_1^{\rm NP}(m_b) \\ c_2^{\rm NP}(m_b) \end{pmatrix} = U^{(\rm LO)} \begin{pmatrix} c_1^{\rm NP}(M_W) \\ c_2^{\rm NP}(M_W) \end{pmatrix}. \tag{5.3}$$

In the above relation, $U^{(\rm LO)}$ can be obtained as it is customarily done [25].

In what follows, the detail of the numerical investigation is outlined; for definitiveness, one of the six categories in Table I is discussed, while the other five cases are analyzed in a similar way. We first generate a value of $a_1(m_b)$ randomly from the range

$$0 < a_1(m_b) < a_1^{\rm max}, \tag{5.4}$$

with the upper limit selected to cover the relevant parameter range, $a_1^{\rm max} = 1.15$. As a next step, we generate Br^{ij} with $(i,j) = (+,-), (0,0), (0,-)$, V_{cb}, f_T, f_C, and $f^{B\to D,+-}$ as random Gaussian numbers. Here, $f_T(f_C)$ represents a decay constant for a meson that is emitted from the W boson in the color-allowed (color-suppressed) tree process, while $f^{B\to D,+-}$ represents heavy-to-heavy form factors with proper charge assignment in the final state. The central value and uncertainty for Br^{ij} are given in Table I, while those for the other ones are given in Table II of Appendix C.

With the generated parameters, $\mathrm{Re}(\bar{a}_2), \mathrm{Im}(\bar{a}_2)$, and δ' are computed from Eqs. (2.16)–(2.18) or (2.29)–(2.31), with the choice of overall signs in Eqs. (2.17) and (2.30) and the twofold ambiguity of δ' in Eqs. (2.18) and (2.31) selected randomly with a large sampling number. At this stage, we properly remove the parameter set that does not satisfy Eqs. (2.19)–(2.21) or (2.32)–(2.34) in such a way to ensure the existence of the solutions.

It should be noted that $c_1^{\rm NP}(M_W)$ and $c_2^{\rm NP}(M_W)$ are not simultaneously determined by the given value of $a_1(m_b)$ in Eq. (5.1). In view of this aspect, $c_2^{\rm NP}(M_W)$ is computed from the fixed values of $a_1(m_b)$ and $c_1^{\rm NP}(M_W)$, via the relation in Eq. (5.1), i.e.,

$$c_2^{\rm NP}(M_W) = \frac{a_1(m_b) - a_1^{\rm SM}(m_b) - (U_{11}^{(\rm LO)} + U_{21}^{(\rm LO)}/3) c_1^{\rm NP}(M_W)}{U_{12}^{(\rm LO)} + U_{22}^{(\rm LO)}/3}. \tag{5.5}$$

This means that the possible values of $c_2^{\rm NP}(M_W)$ are scanned in the parameter space. For $a_1^{\rm SM}(m_b)$, its imaginary part arises solely from the radiative correction [1,7] and is negligible to high accuracy for our current purpose.

The $\tau(B^+)/\tau(B_d)$ in the presence of NP can be evaluated from $c_2^{\rm NP}(M_W)$ and $c_1^{\rm NP}(M_W)$. In analyzing the lifetime ratio, input parameters including the heavy-quark mass and power correction parameters in the heavy quark effective theory (HQET) are adopted from Ref. [47] in the kinetic scheme [48,49]. As to the value in the SM at NLO QCD, the recent result [26] is

$$\left[\frac{\tau(B^+)}{\tau(B_d^0)}\right]_{\rm SM,NLO} = 1.081^{+0.014}_{-0.016}. \tag{5.6}$$

We adopt the central value and the larger side of the uncertainty in Eq. (5.6). For the interference terms between SM and NP contributions, as well as the terms purely originating from NP, we consider the LO accuracy in QCD corrections with $c_1^{\rm SM}(m_b) = 1.098$ and $c_2^{\rm SM}(m_b) = -0.231$, which can be obtained with Ref. [25]. The same accuracy is used in the numerical analysis of $B_d - \bar{B}_d$ mixing. For the charm-quark mass input, the $\bar{m}_c(m_c)$ is converted to one at 3 GeV via RunDec [58], leading to $m_c = 0.985$ GeV.

One can define χ^2 to impose the constraints on the parameters of the NP scenario [22]. In our analysis, the following χ^2 functions are introduced:

$$\chi^2_{(\rm A)} = \sum_{(i,j)=(+,-)}^{(0,0),(0,-)} \left(\frac{\mathrm{Br}^{ij} - \mathrm{Br}^{ij}_{\rm cent}}{\delta \mathrm{Br}^{ij}}\right)^2 + \left(\frac{|V_{cb}| - |V_{cb}|_{\rm cent}}{\delta |V_{cb}|}\right)^2 + \left(\frac{f_T - f_{T,\rm cent}}{\delta f_T}\right)^2 + \left(\frac{f_C - f_{C,\rm cent}}{\delta f_C}\right)^2 + \left(\frac{f^{B\to D,+-} - f^{B\to D,+-}_{\rm cent}}{\delta f^{B\to D,+-}}\right)^2, \tag{5.7}$$

$$\chi^2_{(\rm B)} = \chi^2_{(\rm A)} + \left\{\frac{[\tau(B^+)/\tau(B_d)]_{\rm th} - [\tau(B^+)/\tau(B_d)]_{\rm exp}}{\sqrt{\delta[\tau(B^+)/\tau(B_d)]^2_{\rm th} + \delta[\tau(B^+)/\tau(B_d)]^2_{\rm exp}}}\right\}^2. \tag{5.8}$$

It should be noted that $\chi^2_{(A)}$ does not include the $\tau(B^+)/\tau(B^+)$ constraint, while $\chi^2_{(B)}$ does. The above two quantities are evaluated based on the parameters generated from the Gaussian distribution, as described before. This analysis is not the minimization procedure and instead scans the parameter region [22] in the present case, including rescattering for the exclusive decays. In Eq. (5.7), $(\cdots)_{\rm cent}$ represents the central value of relevant quantities,

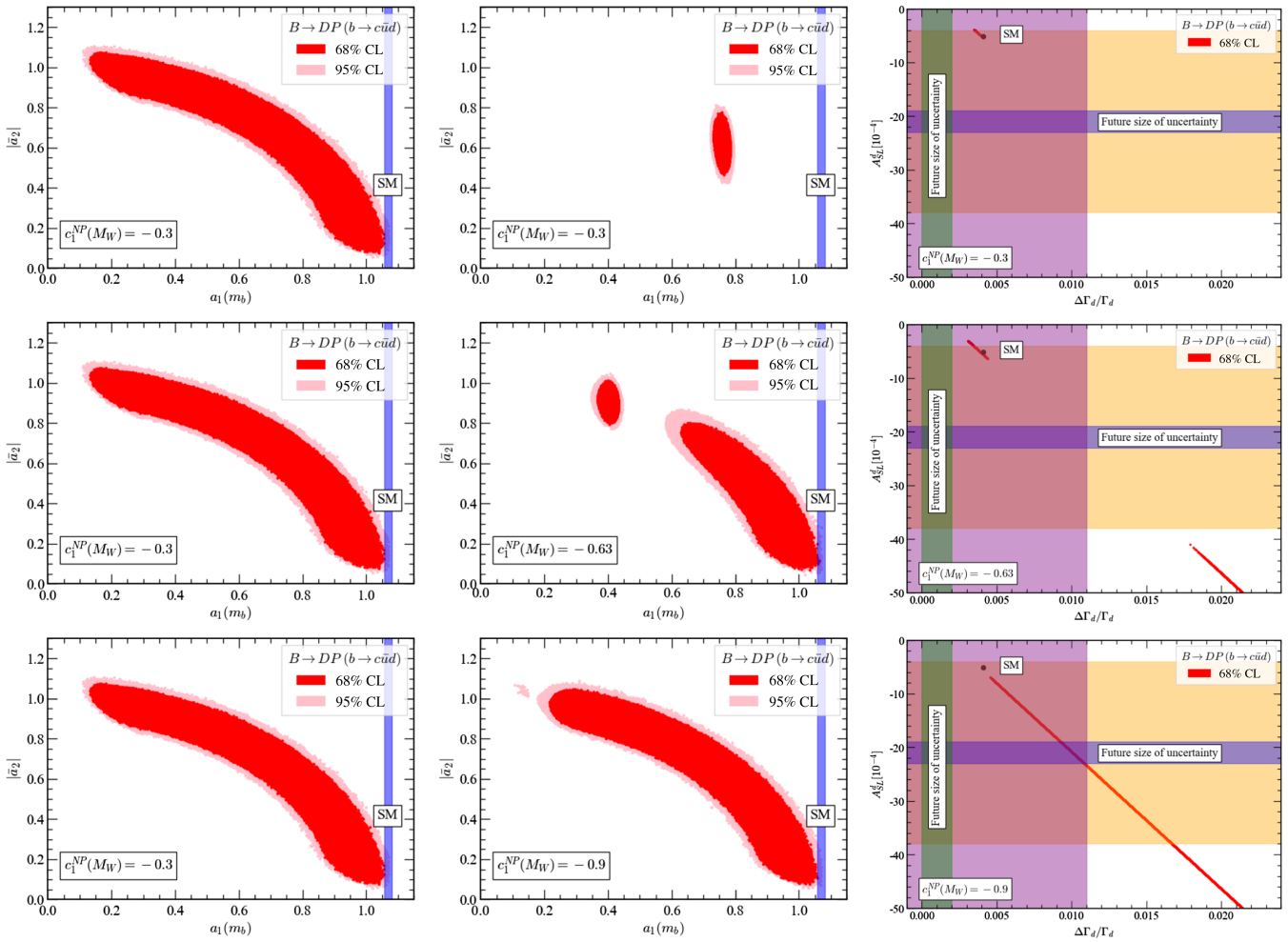

FIG. 1. Left column: parameter regions that satisfy the phenomenological constraints without $\tau(B^+)/\tau(B_d)$, for the $a_1(m_b)$ versus $|\tilde{a}_2|$ plane. Middle column: parameter regions that satisfy the constraints including $\tau(B^+)/\tau(B_d)$ in addition to those in left column. See the main text for details. The blue bands represent $a_1^{\rm SM}(m_b) = 1.070 \pm 0.012$ [16], universal to the high precision [7] at NNLO. The red and pink points represent the regions where the constraints are satisfied at 1σ and 2σ confidence levels, respectively. Right column: predictions for $\Delta\Gamma_d/\Gamma_d$ and $\mathcal{A}_{\rm SL}^d$ that satisfy the phenomenological constraints including the $\tau(B^+)/\tau(B_d)$ data. The central value for the SM prediction is given by a black point, while the yellow and light purple bands represent the current HFLAV 1σ ranges [62]. The future experimental uncertainties [63,64], where the central values are assumed to remain unchanged from those in HFLAV [62], are represented as purple and green bands. The upper, middle, and lower rows, respectively, represent the results with $c_1^{\rm NP}(M_W) = -0.3, -0.63$, and -0.9.

while $\delta(\cdots)$ stands for its uncertainty given in Tables I and II. The heavy-to-light form factors are set to their central values and not included in Eqs. (5.7) and (5.8) since the branching ratios have rather weak dependence on those quantities, which are accompanied by SU(3) breaking, as given in $\Delta_{DP}^{(2)}$ in Eq. (A19). As for $|V_{cb}|_{\rm cent}$ and $\delta|V_{cb}|$ in Eq. (5.7), we use the value obtained by the exclusive fitting [51] exhibited in Table II. In Eq. (5.8), the larger theoretical uncertainty of the lifetime ratio in Eq. (5.6) is adopted as $\delta[\tau(B^+)/\tau(B_d)]_{\rm th} = 0.016$. The experimental data from the Heavy Flavor Averaging Group (HFLAV) are set to $[\tau(B^+)/\tau(B_d)]_{\rm exp} = 1.078$ and $\delta[\tau(B^+)/\tau(B_d)]_{\rm exp} = 0.004$.

Assembling the mentioned procedure, $\chi^2_{(A)}$ and $\chi^2_{(B)}$ can be calculated with d.o.f. equal to 7 and 8, respectively. The values of $\chi^2_{(A)} \approx 8.18 (\chi^2_{(A)} \approx 14.3)$ and $\chi^2_{(B)} \approx 9.30 (\chi^2_{(B)} \approx 15.8)$ are used to determine the 1σ (2σ) region that satisfies the phenomenological constraints. Furthermore, $\Delta\Gamma_d$ and $\mathcal{A}_{\rm SL}^d$ are evaluated as resulting predictions satisfying the mentioned constraints. The explained routine is repeated with a number of random values for $a_1(m_b)$ in Eq. (5.4). Furthermore, different fixed values of $c_1^{\rm NP}(M_W)$ are investigated in the following results.

The input parameters to compute the $B_d^0 - \bar{B}_d^0$ mixing are displayed in Table II. The bottom-quark mass and charm-quark mass are fixed to $\bar{m}_b(m_b)$ and $\bar{m}_c(m_b)$, respectively, while the top-quark mass is set to $\bar{m}_t(m_t)$. In order to get

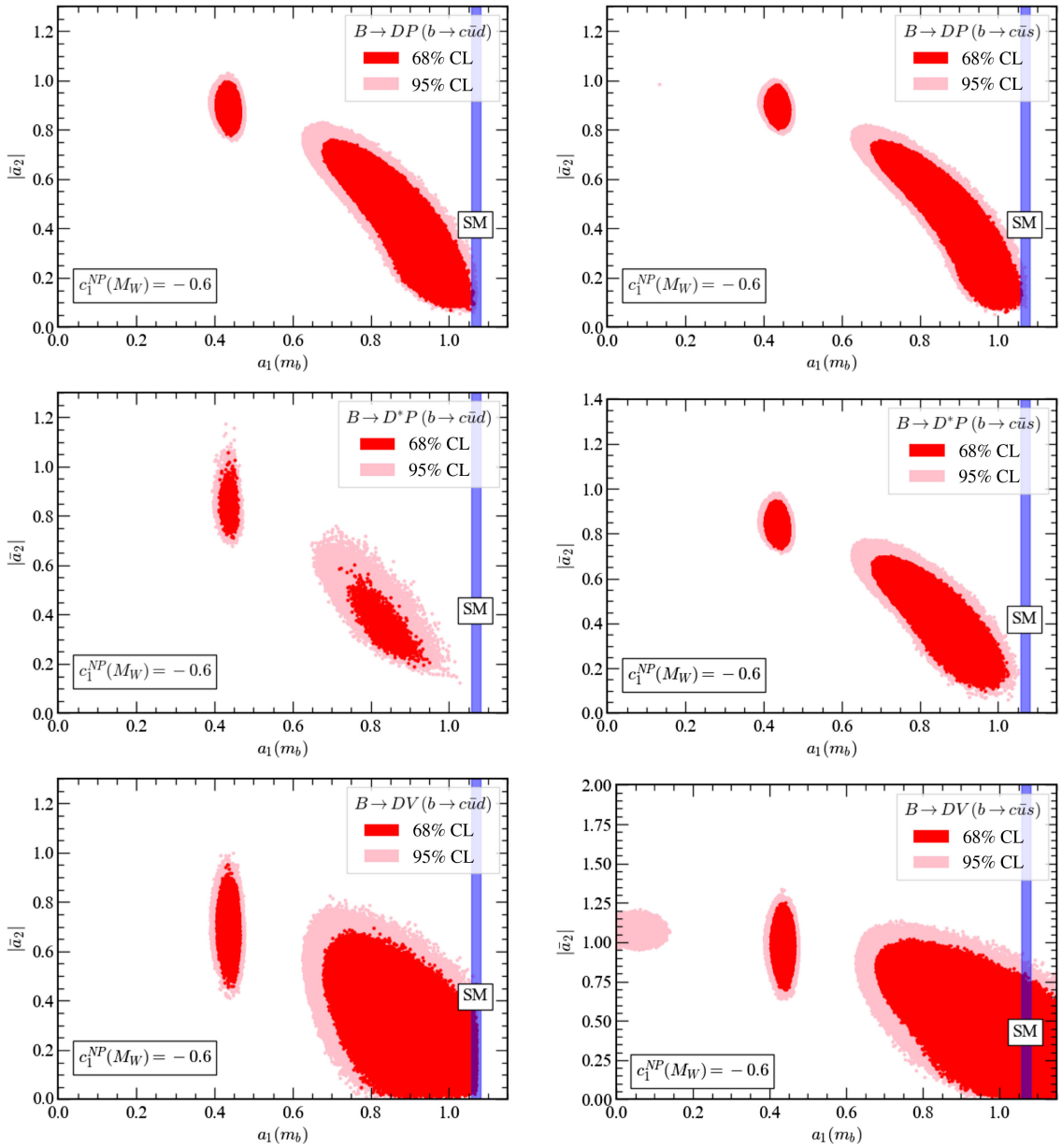

FIG. 2. Plots similar to the middle column of Fig. 1 except that six different types of final states are analyzed, with fixed $c_1^{\mathrm{NP}}(M_W) = -0.6$. The constraint of the $\tau(B^+)/\tau(B_d)$ data is included in the individual plots.

$\bar{m}_c(m_b)$ and $\bar{m}_t(m_t)$, the respective inputs are converted via RunDec [58], giving $\bar{m}_c(m_b) = 0.942$ GeV and $\bar{m}_t(m_t) = 163.3$ GeV. This procedure is used to compute the contributions induced by NP with the operator basis in Appendix B 2.[4] As for the SM contribution, we use [61]

$$[\Delta\Gamma_d]_{\mathrm{SM}} = (2.7 \pm 0.4) \times 10^{-3}\ \mathrm{ps}^{-1},$$
$$[\mathcal{A}_{\mathrm{SL}}^d]_{\mathrm{SM}} = -(5.1 \pm 0.5) \times 10^{-4}. \tag{5.9}$$

[4]In Ref. [59] (see also the review in Ref. [60]), the new operator basis was discussed. This leads to a difference in which operator is treated as the leading power one.

For the experimental data of $\Delta\Gamma_d/\Gamma_d$ and $\mathcal{A}_{\mathrm{SL}}^d$, the current values are given by HFLAV [62],

$$\left[\frac{\Delta\Gamma_d}{\Gamma_d}\right]_{\mathrm{HFLAV}} = 0.001 \pm 0.010,$$
$$[\mathcal{A}_{\mathrm{SL}}^d]_{\mathrm{HFLAV}} = -0.0021 \pm 0.0017. \tag{5.10}$$

For the latter two quantities, the experimental uncertainties are much larger than the theoretical central values in Eq. (5.9). As for the future experimental projection, an improvement of (statistical) uncertainty is expected for $\Delta\Gamma_d/\Gamma_d$ via upgrade II in the LHCb measurement [63].

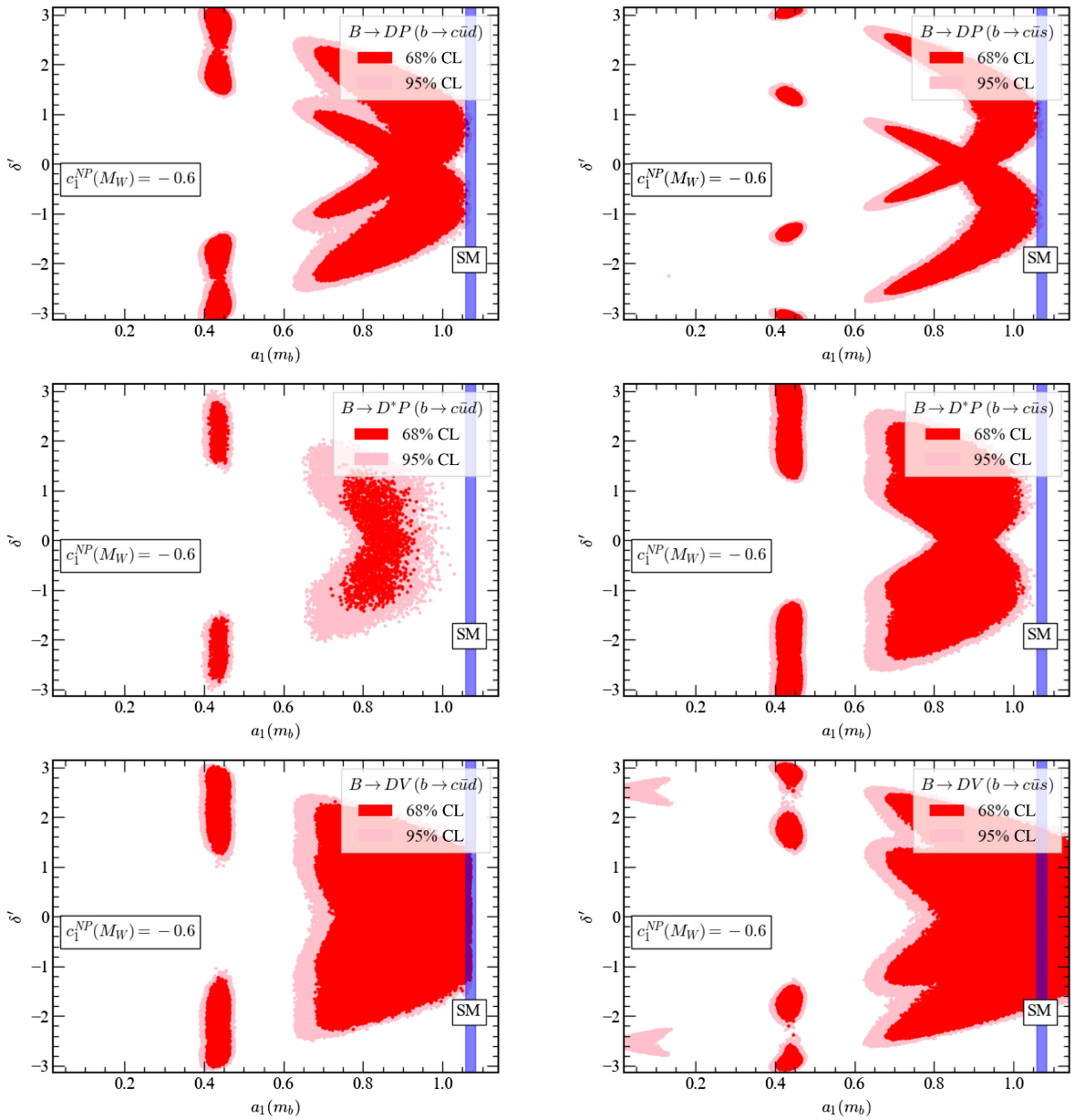

FIG. 3. Plots similar to Fig. 2 with the vertical axes replaced by δ', the rescattering angle. The constraint of the $\tau(B^+)/\tau(B_d)$ data is included in the individual plots.

Moreover, the uncertainty of $\mathcal{A}^d_{\rm SL}$ is also reduced due to Runs 1–5 (300 fb^{-1}) data at LHCb [64]. Those future projections read

$$\delta\left(\frac{\Delta\Gamma_d}{\Gamma_d}\right)_{\rm future} = 1 \times 10^{-3},$$
$$\delta(\mathcal{A}^d_{\rm SL})_{\rm future} = 2 \times 10^{-4}. \tag{5.11}$$

The above numerics are adopted as the reference values, assuming that the corresponding central values are unchanged from the current HFLAV data.

In order to exhibit how the $\tau(B^+)/\tau(B^+)$ constraint works, we consider three choices of parameters: $c_1^{\rm NP}(M_W) = -0.3, -0.63$, and -0.9. For illustrative purposes, we first take $B \to DP$ for the $b \to c\bar{u}d$ transition. In the left column of Fig. 1, the allowed parameter regions that satisfy the phenomenological constraints *without* the $\tau(B^+)/\tau(B_d)$ data based on Eq. (5.7) are exhibited for the $a_1(m_b)$ versus $|\bar{a}_2|$ plane. These three plots are to be contrasted with those in the middle column in Fig. 1, which account for the $\tau(B^+)/\tau(B_d)$ constraint in addition to those in left column, based on Eq. (5.8). The middle column panels give an improved result compared with Ref. [16], since the constraint of the lifetime ratio is included.

Comparing the left and middle columns of Fig. 1, one immediately finds that how stringent the lifetime constraint is depends crucially on the choice of the NP parameters. Among the displayed results, $c_1^{\rm NP}(M_W) = -0.3$, corresponding to the upper-left and upper-middle panels, gives a result that is most significantly constrained by the lifetime ratio. However, for the case of $c_1^{\rm NP}(M_W) = -0.9$, the lifetime constraint works weakly, as shown in the lower-left and lower-middle panels in Fig. 1.

Furthermore, in the right column of Fig. 1, the resulting predictions for $B_d^0 - \bar{B}_d^0$ mixing are exhibited. The results are based on the parameter region that satisfies the phenomenological constraints including $\tau(B^+)/\tau(B_d)$ for 68% CL. In order to compute $\Delta\Gamma_d/\Gamma_d$, the formula in Eq. (4.11) and the HFLAV lifetime of B_d in Eq. (C1) are used. Among the plotted choices of $c_1^{\rm NP}(M_W)$, -0.3 gives a prediction that is closest to the SM, while the deviation range from the SM becomes wider for $c_1^{\rm NP}(M_W) = -0.63$ and -0.9. As can be seen in the middle-right and lower-right panels, the resulting variation ranges are larger than the future size of the experimental uncertainties. Hence, we conclude that this type of scenario, where NP contributions are involved in the presence of rescattering, can be testable via future LHCb measurements. In Fig. 2, the results similar to the middle column of Fig. 1, except that six different types of final states are analyzed with fixed $c_1^{\rm NP}(M_W) = -0.6$. As shown in the plots, the patterns of the constrained parameter regions are different individually. Moreover, plots showing the correlation between $a_1(m_b)$ and δ' are displayed in Fig. 3. It should be noted that the constraint from $\tau(B^+)/\tau(B_d)$ is included in all plots in Figs. 2 and 3. As can be seen from the plots, the rescattering angle gives a pattern characterized by the sign choice and twofold ambiguity, as explained before.

VI. SUMMARY

In this work, the phenomenological analysis of $B \to DM$ decays in the presence of quasielastic rescattering was carried out via a model-independent manner, which in general includes the contributions of NP. The rescattering phase and coefficient of the color-suppressed tree diagram (denoted as $a_2^{\rm eff}$) were analytically constrained by the experimental data of the branching ratios and theoretical inputs such as form factors. These feasible restrictions were applied for the final states with $S = -1, I_z = 0$ and $S = 1, I_z = -1$, where the branching ratios are altered only by the relative phase between δ_6 and $\delta_{\overline{15}}$. The numerical results were given for the two-body nonleptonic decays of $\bar{B}_{(s)} \to D_{(s)}^{(*)} P$ and $\bar{B}_{(s)} \to D_{(s)} V$ in a systematic way. For both $b \to c\bar{u}s$ and $b \to c\bar{u}d$, the set of the constraining relations were obtained, where the latter includes the SU(3) breaking from the decay constants and masses.

We included the B-meson lifetime ratio to impose constraints on the phenomenological discussion of $B \to DM$ in the presence of the quasielastic rescattering. These observables are correlated with $B \to DM$ due to the nonleptonic Wilson coefficients. For the NP contributions, we considered the model-independent modification of the Wilson coefficients for the current-current operators, denoted as c_1 and c_2. Depending on the parameter space, we found that the lifetime ratio can give a stringent bound on the rescattering and NP parameters, as the NP contribution modifies Pauli interference, affecting the lifetime difference between B^+ and B_d. Meanwhile, it was also found that some specific parameter sets, such as $c_1^{\rm NP}(M_W) = -0.9$ with $c_2^{\rm NP}(M_W)$ varied, are rather weakly constrained by the lifetime ratio. Based on this methodology, the allowed parameter regions for $a_1(m_b)$, $a_2^{\rm eff}$, and δ' were discussed, where the correlations between them were clarified numerically.

Furthermore, the width difference and CP violation in $B_d^0 - \bar{B}_d^0$ mixing, where the latter is measured via the semileptonic asymmetry, were analyzed as predictions that satisfy the phenomenological constraints, such as $\tau(B^+)/\tau(B_d)$ and $\mathrm{Br}[B \to DM]$. We found that for some specific choices of Wilson coefficients from NP, the two mentioned observables can be considerably shifted from the SM predictions. This deviation size is larger than the future uncertainties in the LHCb experiment [63,64], and thus the considered scenario, in which the rescattering and beyond-the-SM contributions are involved, is testable via future measurements.

ACKNOWLEDGMENTS

The authors would like to thank Hai-Yang Cheng for providing the *Mathematica* code. Furthermore, the authors are grateful to Boris Blok and Xiaodong Shi for useful comments. The work of H. U. is supported by the National Science Foundation of China under Grant No. 12405111 and the Seeds Funding of Jilin University.

DATA AVAILABILITY

No data were created or analyzed in this study.

APPENDIX A: DETERMINATIONS OF $\bar{a}_2$ AND δ' FROM EXPERIMENTAL DATA

1. $b \to c\bar{u}s$

Here, the derivations of Eqs. (2.16)–(2.18) are given. The coefficients in Eq. (2.14) are defined by

$$N^T_{DK} = \frac{G_F}{\sqrt{2}}(m_B^2 - m_D^2) f_K F_0^{BD}(m_K^2), \qquad N^C_{DK} = \frac{G_F}{\sqrt{2}}(m_B^2 - m_K^2) f_D F_0^{BK}(m_D^2), \tag{A1}$$

$$N^T_{D^*K} = \frac{G_F}{\sqrt{2}} 2 m_{D^*} f_K A_0^{BD^*}(m_K^2), \qquad N^C_{D^*K} = \frac{G_F}{\sqrt{2}} 2 m_{D^*} f_{D^*} F_+^{BK}(m_{D^*}^2), \tag{A2}$$

$$N^T_{DK^*} = \frac{G_F}{\sqrt{2}} 2 m_{K^*} f_{K^*} F_+^{BD}(m_{K^*}^2), \qquad N^C_{DK^*} = \frac{G_F}{\sqrt{2}} 2 m_{K^*} f_D A_0^{BK^*}(m_D^2). \tag{A3}$$

In what follows, we consider B-meson decays into two pseudoscalars for definitiveness, unless otherwise specified. In the presence of quasielastic rescattering, amplitudes are given by

$$\mathcal{A}_f^{+-} = N^T_{DK} a_1 \left(\frac{1 + e^{i\delta'}}{2} + \bar{a}_2 \frac{1 - e^{i\delta'}}{2} \right) e^{i\delta_{\overline{15}}}, \tag{A4}$$

$$\mathcal{A}_f^{00} = N^T_{DK} a_1 \left(\frac{1 - e^{i\delta'}}{2} + \bar{a}_2 \frac{1 + e^{i\delta'}}{2} \right) e^{i\delta_{\overline{15}}}, \tag{A5}$$

$$\mathcal{A}_f^{0-} = N^T_{DK} a_1 (1 + \bar{a}_2). \tag{A6}$$

One can find that dependence on the heavy-to-light form factors is absorbed by $\bar{a}_2$, so that Eqs. (A4)–(A6) can be evaluated solely by the heavy-to-heavy form factors. This is not the case for $b \to c\bar{u}d$ decays, as explicitly shown later.

It should be noted that the overall phase in Eqs. (A4)–(A6) cancels out when being squared for the evaluation of decay rates. By substituting Eqs. (A4)–(A6) into Eq. (2.9), one can obtain the branching ratios

$$\frac{\mathrm{Br}^{+-}}{\mathcal{N}_{DK}} = \frac{1 + \cos\delta'}{2} + |\bar{a}_2|^2 \frac{1 - \cos\delta'}{2} + \mathrm{Im}(\bar{a}_2) \sin\delta', \tag{A7}$$

$$\frac{\mathrm{Br}^{00}}{\mathcal{N}_{DK}} = \frac{1 - \cos\delta'}{2} + |\bar{a}_2|^2 \frac{1 + \cos\delta'}{2} - \mathrm{Im}(\bar{a}_2) \sin\delta', \tag{A8}$$

$$\frac{\tau^{+-}}{\tau^{0-}} \frac{\mathrm{Br}^{0-}}{\mathcal{N}_{DK}} = 1 + |\bar{a}_2|^2 + 2\mathrm{Re}(\bar{a}_2), \tag{A9}$$

where the following objects are introduced:

$$\mathcal{N}_{DK} = \frac{\tau_P p_{\mathrm{cm}}[P \to M_1 M_2]}{8\pi m_P^2} |V_{cb} V_{us}^*|^2 (N^T_{M_1 M_2})^2 |a_1|^2, \tag{A10}$$

$$\mathcal{N}_{D^*K} = \frac{\tau_P p^3_{\mathrm{cm}}[P \to M_1^* M_2]}{8\pi m_{M_1^*}^2} |V_{cb} V_{us}^*|^2 (N^T_{M_1^* M_2})^2 |a_1|^2, \tag{A11}$$

$$\mathcal{N}_{DK^*} = \frac{\tau_P p^3_{\mathrm{cm}}[P \to M_1 M_2^*]}{8\pi m_{M_2^*}^2} |V_{cb} V_{us}^*|^2 (N^T_{M_1 M_2^*})^2 |a_1|^2. \tag{A12}$$

Furthermore, the following variables are introduced:

$$A_{DK} = 2\,\mathrm{Im}(\bar{a}_2), \tag{A13}$$

$$B_{DK} = 1 - |\bar{a}_2|^2, \tag{A14}$$

$$\omega_{DK} = \begin{cases} \mathrm{Arcsin}\left(\frac{B_{DK}}{\sqrt{A_{DK}^2 + B_{DK}^2}} \right) & \text{for } A_{DK} \geq 0, \\ \pi \mathrm{sign}(B_{DK}) - \mathrm{Arcsin}\left(\frac{B_{DK}}{\sqrt{A_{DK}^2 + B_{DK}^2}} \right) & \text{for } A_{DK} < 0. \end{cases} \tag{A15}$$

By rewriting the three relations in Eqs. (A7)–(A9) in terms of $\mathrm{Re}(\bar{a}_2), \mathrm{Im}(\bar{a}_2)$ and δ', one can obtain Eqs. (2.16)–(2.18) if the conditions of Eqs. (2.19)–(2.21) are satisfied.

2. $b \to c\bar{u}d$

The derivation of Eqs. (2.29)–(2.31) is given in a way similar to $b \to c\bar{u}s$ decays, except that the SU(3) breaking should be taken into account. We introduce parameters related to SU(3) breaking,

$$z_{DP} = \frac{f_{D_s} f_\pi}{f_D f_K}, \qquad r_{DP} = \frac{p_{\mathrm{cm}}[\bar{B}_s^0 \to D^0 \bar{K}^0]}{p_{\mathrm{cm}}[\bar{B}_s^0 \to D_s^+ \pi^-]}, \tag{A16}$$

$$z_{D^*P} = \frac{f_{D_s^*} f_\pi}{f_{D^*} f_K}, \qquad r_{D^*P} = \left(\frac{m_{D_s^{*+}}}{m_{D^{*0}}} \right)^2 \frac{p^3_{\mathrm{cm}}[\bar{B}_s^0 \to D^{*0} \bar{K}^0]}{p^3_{\mathrm{cm}}[\bar{B}_s^0 \to D_s^{*+} \pi^-]}, \tag{A17}$$

$$z_{DV} = \frac{f_{D_s} f_\rho}{f_D f_{K^*}}, \qquad r_{DV} = \left(\frac{m_{\rho^+}}{m_{K^{*0}}}\right)^2 \frac{p^3_{\rm cm}[\bar{B}^0_s \to D^0 \bar{K}^{*0}]}{p^3_{\rm cm}[\bar{B}^0_s \to D^+_s \rho^-]}, \tag{A18}$$

$$\Delta^{(1)}_{DP} = \left(\frac{N^{D^+_s\pi^-}_T}{N^{D^0\pi^-}_T}\frac{N^{D^0\pi^-}_C}{N^{D^0\bar{K}^0}_C}\right)^{-1} \frac{\mathcal{N}_{D^+_s\pi^-}}{\mathcal{N}_{D^0\pi^-}}\frac{\tau^{0-}}{\tau^{+-}} - 1,$$
$$\Delta^{(2)}_{DP} = \frac{1}{z^2_{DP}}\frac{N^{D^+_s\pi^-}_T}{N^{D^0\pi^-}_T}\frac{N^{D^0\pi^-}_C}{N^{D^0\bar{K}^0}_C} - 1, \tag{A19}$$

$$\Delta^{(3)}_{DP} = \frac{z^2_{DP}}{r_{DP}} - 1, \qquad \Delta^{(4)}_{DP} = z^2_{DP}\left(\frac{N^{D^+_s\pi^-}_T}{N^{D^0\pi^-}_T}\frac{N^{D^0\pi^-}_C}{N^{D^0\bar{K}^0}_C}\right)^{-2} - 1,$$
$$\Delta^{(5)}_{DP} = \frac{1}{z^2_{DP}} - 1. \tag{A20}$$

On the basis of the previously introduced notations, the decay amplitudes for $b \to c\bar{u}d$ processes with FSIs can be given as follows:

$$\mathcal{A}_f[\bar{B}^0_s \to D^+_s\pi^-] = N^T_{D^+_s\pi^-} a_1 \left(\frac{1+e^{i\delta'}}{2} + z_{DP}\bar{a}_2\frac{1-e^{i\delta'}}{2}\right)e^{i\delta_{\overline{15}}}, \tag{A21}$$

$$\mathcal{A}_f[\bar{B}^0_s \to D^0\bar{K}^0] = \frac{N^T_{D^+_s\pi^-}}{z_{DP}} a_1 \left(\frac{1-e^{i\delta'}}{2} + z_{DP}\bar{a}_2\frac{1+e^{i\delta'}}{2}\right)e^{i\delta_{\overline{15}}}, \tag{A22}$$

$$\mathcal{A}_f[B^- \to D^0\pi^-] = N^T_{D^0\pi^-} a_1 \left(1 + \frac{N^T_{D^+_s\pi^-}}{N^T_{D^0\pi^-}}\frac{N^C_{D^0\pi^-}}{N^C_{D^0\bar{\pi}^0}}\bar{a}_2\right). \tag{A23}$$

Since $\bar{a}_2$ is defined so as to absorb $N^{D^0\bar{K}^0}_C$, the overall dependence on heavy-to-light form factors vanishes in Eqs. (A21) and (A22), whereas it is included as a prefactor of $\bar{a}_2$ in Eq. (A23). Furthermore, the following parameters are introduced:

$$A_{DP} = 2z_{DP}\,\mathrm{Im}(\bar{a}_2), \tag{A24}$$

$$B_{DP} = 1 - z^2_{DP}|\bar{a}_2|^2. \tag{A25}$$

The expression of ω_{DP} is found by the replacement of $A_{DK} \to A_{DP}$ and $B_{DK} \to B_{DP}$ for ω_{DP} in Eq. (A15).

By using the SU(3)-breaking parameters, one can write relations similar to Eqs. (A7)–(A9) in the case of $b \to c\bar{u}d$ decays, which is omitted here. These relations are solved with respect to the QCDF approach and the rescattering parameters, leading to Eqs. (2.29)–(2.31) under the conditions of Eqs. (2.32)–(2.34).

APPENDIX B: EFFECTIVE WEAK OPERATORS AND MATRIX ELEMENTS

1. $\Delta B = 1$ processes

The effective operators for the weak Hamiltonian in Eq. (2.1) are defined by [22]

$$Q^{\bar{q}_2 q_3}_1 = (\bar{c}^\alpha b^\alpha)_{\rm V-A}(\bar{q}^\beta_3 q^\beta_2)_{\rm V-A}, \qquad Q^{\bar{q}_2 q_3}_2 = (\bar{c}^\alpha b^\beta)_{\rm V-A}(\bar{q}^\beta_3 q^\alpha_2)_{\rm V-A}, \tag{B1}$$

$$Q^{q_3}_3 = \bar{q}^\alpha_3 b^\alpha)_{\rm V-A}(\bar{q}^\beta q^\beta)_{\rm V-A}, \qquad Q^{q_3}_4 = (\bar{q}^\alpha_3 b^\beta)_{\rm V-A}(\bar{q}^\beta q^\alpha)_{\rm V-A}, \tag{B2}$$

$$Q^{q_3}_5 = \bar{q}^\alpha_3 b^\alpha)_{\rm V-A}(\bar{q}^\beta q^\beta)_{\rm V+A}, \qquad Q^{q_3}_6 = (\bar{q}^\alpha_3 b^\beta)_{\rm V-A}(\bar{q}^\beta q^\alpha)_{\rm V+A}, \tag{B3}$$

$$Q^{q_3}_8 = \frac{g_s}{8\pi^2} m_b \bar{q}^\alpha_3 \sigma^{\mu\nu}(1+\gamma_5) t^a_{\alpha\beta} b^\beta G^a_{\mu\nu}, \tag{B4}$$

where sums over colors denoted by α and β and flavor indices are taken implicitly. For $(\cdots)_{\rm V\pm A}$, the current is represented as $\gamma^\mu(1 \pm \gamma_5)$.

As for B-meson decays into an exclusive hadronic state, matrix elements relevant for our work are parametrized by form factors [1,65],

$$\langle P(p')|c\gamma^\mu b|B(p)\rangle = F^{BP}_+(q^2)\left[(p+p')^\mu - \frac{m^2_B - m^2_D}{q^2}q^\mu\right] + F^{BP}_0(q^2)\frac{m^2_B - m^2_D}{q^2}q^\mu, \tag{B5}$$

$$\langle V(p',\epsilon)|c\gamma^\mu\gamma_5 b|B(p)\rangle = \left[(m_B + m_V)\epsilon^{*\mu}A^{BV}_1(q^2) - \frac{\epsilon^*\cdot q}{m_B+m_V}(p+p')^\mu A^{BV}_2(q^2) - 2m_V\frac{\epsilon^*\cdot q}{q^2}q^\mu A^{BV}_3(q^2)\right] + 2m_V\frac{\epsilon^*\cdot q}{q^2}q^\mu A^{BV}_0(q^2), \tag{B6}$$

$$A^{BV}_3(q^2) = \frac{m_B + m_V}{2m_V}A^{BV}_1(q^2) - \frac{m_B - m_V}{2m_V}A^{BV}_2(q^2), \tag{B7}$$

where P and V are a pseudoscalar and vector meson, respectively, with $q = p - p'$.

2. $\Delta B = 0$ processes

Operators for the $\Delta B = 0$ transition are divided into two-quark and four-quark operators. For the former, the dimension-five operators are defined by [23]

$$O_\pi = -\bar{b}_v (iD_\mu)(iD^\mu) b_v, \tag{B8}$$

$$O_G = \bar{b}_v (iD_\mu)(iD_\nu)(-i\sigma^{\mu\nu}) b_v, \tag{B9}$$

where $b(x) = e^{-im_b v\cdot x} b_v(x)$. The matrix elements for the above operators are

$$\mu_\pi^2 = \frac{\langle B|O_\pi|B\rangle}{2m_B}, \qquad \mu_G^2 = \frac{\langle B|O_G|B\rangle}{2m_B}. \tag{B10}$$

The matrix elements in Eq. (B10) enter our analysis in the denominator of the second term in Eq. (3.2). As for the four-quark operators, we introduce [29]

$$Q_1^q = (\bar{b}q)_{\mathrm{V-A}} (\bar{q}b)_{\mathrm{V-A}}, \tag{B11}$$

$$Q_2^q = (\bar{b}q)_{\mathrm{S-P}} (\bar{q}b)_{\mathrm{S+P}}, \tag{B12}$$

$$Q_3^q = \bar{b}t^a q)_{\mathrm{V-A}} (\bar{q}t^a b)_{\mathrm{V-A}}, \tag{B13}$$

$$Q_4^q = (\bar{b}t^a q)_{\mathrm{S-P}} (\bar{q}t^a b)_{\mathrm{S+P}}, \tag{B14}$$

where $(\cdots)_{\mathrm{S\pm P}}$ represents a bilinear of the form $(1 \pm \gamma_5)$. The matrix elements for Eqs. (B11)–(B14) are defined by

$$\langle B_q|Q_1^q|B_q\rangle = f_{B_q}^2 m_{B_q}^2 B_1, \tag{B15}$$

$$\langle B_q|Q_2^q|B_q\rangle = f_{B_q}^2 m_{B_q}^2 B_2, \tag{B16}$$

$$\langle B_q|Q_3^q|B_q\rangle = f_{B_q}^2 m_{B_q}^2 \epsilon_1, \tag{B17}$$

$$\langle B_q|Q_4^q|B_q\rangle = f_{B_q}^2 m_{B_q}^2 \epsilon_2. \tag{B18}$$

3. $\Delta B = 2$ processes

Effective operators relevant for $B_d^0 - \bar{B}_d^0$ mixing are given by dimension-six operators,

$$\mathcal{O}_1^d = (\bar{b}^\alpha d^\alpha)_{\mathrm{V-A}} (\bar{b}^\beta d^\beta)_{\mathrm{V-A}}, \quad \mathcal{O}_2^d = (\bar{b}^\alpha d^\alpha)_{\mathrm{S-P}} (\bar{b}^\beta d^\beta)_{\mathrm{S-P}}, \tag{B19}$$

$$\mathcal{O}_3^d = (\bar{b}^\alpha d^\beta)_{\mathrm{S-P}} (\bar{b}^\beta d^\alpha)_{\mathrm{S-P}}, \quad \mathcal{O}_4^d = (\bar{b}^\alpha d^\alpha)_{\mathrm{S-P}} (\bar{b}^\beta d^\beta)_{\mathrm{S+P}}, \tag{B20}$$

$$\mathcal{O}_5^d = (\bar{b}^\alpha d^\beta)_{\mathrm{S-P}} (\bar{b}^\beta d^\alpha)_{\mathrm{S+P}}, \tag{B21}$$

as well as those giving $1/m_b$ suppressed contributions [42,43],

$$R_1^d = \frac{m_d}{m_b} (\bar{b}^\alpha d^\alpha)_{\mathrm{S-P}} (\bar{b}^\beta d^\beta)_{\mathrm{S+P}}, \tag{B22}$$

$$R_2^d = \frac{1}{m_b^2} [\bar{b}^\alpha \overleftarrow{D}_\rho \gamma^\mu (1-\gamma_5) D^\rho q^\alpha][\bar{b}^\beta \gamma_\mu (1-\gamma_5) q^\beta], \tag{B23}$$

$$R_3^d = \frac{1}{m_b^2} [\bar{b}^\alpha \overleftarrow{D}_\rho (1-\gamma_5) D^\rho q^\alpha][\bar{b}^\beta (1-\gamma_5) q^\beta], \tag{B24}$$

$$R_4^d = \frac{1}{m_b} [\bar{b}^\alpha (1-\gamma_5) iD_\mu q^\alpha][\bar{b}^\beta \gamma^\mu (1-\gamma_5) q^\beta]. \tag{B25}$$

The matrix element of the operators are given by

$$\langle \bar{B}_d|\mathcal{O}_1^d|B_d\rangle = \frac{8}{3} f_{B_d}^2 m_{B_d}^2 B_1^d, \qquad \langle \bar{B}_d|\mathcal{O}_2^d|B_d\rangle = -\frac{5}{3} f_{B_d}^2 m_{B_d}^2 \left(\frac{m_{B_d}}{m_b + m_d}\right)^2 B_2^d, \tag{B26}$$

$$\langle \bar{B}_d|\mathcal{O}_3^d|B_d\rangle = \frac{1}{3} f_{B_d}^2 m_{B_d}^2 \left(\frac{m_{B_d}}{m_b + m_d}\right)^2 B_3^d, \qquad \langle \bar{B}_d|\mathcal{O}_4^d|B_d\rangle = 2 f_{B_d}^2 m_{B_d}^2 \left(\frac{m_{B_d}}{m_b + m_d}\right)^2 B_4^d, \tag{B27}$$

$$\langle \bar{B}_d|\mathcal{O}_5^d|B_d\rangle = \frac{2}{3} f_{B_d}^2 m_{B_d}^2 \left(\frac{m_{B_d}}{m_b + m_d}\right)^2 B_5^d, \tag{B28}$$

$$\langle \bar{B}_d|R_1^d|B_d\rangle = \frac{7}{3} \frac{m_d}{m_b} f_{B_d}^2 m_{B_d}^2 B_{R_1}^d, \qquad \langle \bar{B}_d|R_2^d|B_d\rangle = -\frac{2}{3} f_{B_d}^2 m_{B_d}^2 \left(\frac{m_{B_d}^2}{m_b^2} - 1\right) B_{R_2}^d, \tag{B29}$$

$$\langle \bar{B}_d|R_3^d|B_d\rangle = \frac{7}{6} f_{B_d}^2 m_{B_d}^2 \left(\frac{m_{B_d}^2}{m_b^2} - 1\right) B_{R_3}^d, \qquad \langle \bar{B}_d|R_4^d|B_d\rangle = -f_{B_d}^2 m_{B_d}^2 \left(\frac{m_{B_d}^2}{m_b^2} - 1\right) B_{R_4}^d. \tag{B30}$$

TABLE I. Experimental data of branching ratios of B-meson nonleptonic decays. One for $B^- \to D^0\rho^-$ is from Belle II [46], while the others are extracted from [6].

$B \to DP(b \to c\bar{u}d)$		$B \to DP(b \to c\bar{u}s)$	
$B_s^0 \to D_s^-\pi^+$	$(2.98 \pm 0.14) \times 10^{-3}$	$B^0 \to D^-K^+$	$(2.05 \pm 0.08) \times 10^{-4}$
$B_s^0 \to \bar{D}^0\bar{K}^0$	$(4.3 \pm 0.9) \times 10^{-4}$	$B^0 \to \bar{D}^0K^0$	$(5.5 \pm 0.4) \times 10^{-5}$
$B^+ \to \bar{D}^0\pi^+$	$(4.61 \pm 0.10) \times 10^{-3}$	$B^+ \to \bar{D}^0K^+$	$(3.64 \pm 0.15) \times 10^{-4}$
$B \to D^*P(b \to c\bar{u}d)$		$B \to D^*P(b \to c\bar{u}s)$	
$B_s^0 \to D_s^{*-}\pi^+$	$(1.9^{+0.5}_{-0.4}) \times 10^{-3}$	$B^0 \to D^{*-}K^+$	$(2.16 \pm 0.08) \times 10^{-4}$
$B_s^0 \to \bar{D}^{*0}\bar{K}^0$	$(2.8 \pm 1.1) \times 10^{-4}$	$B^0 \to \bar{D}^{*0}K^0$	$(3.6 \pm 1.2) \times 10^{-5}$
$B^+ \to \bar{D}^{*0}\pi^+$	$(5.17 \pm 0.15) \times 10^{-3}$	$B^+ \to \bar{D}^{*0}K^+$	$(4.19^{+0.31}_{-0.28}) \times 10^{-4}$
$B \to DV(b \to c\bar{u}d)$		$B \to DV(b \to c\bar{u}s)$	
$B_s^0 \to D_s^-\rho^+$	$(6.8 \pm 1.4) \times 10^{-3}$	$B^0 \to D^-K^{*+}$	$(4.5 \pm 0.7) \times 10^{-4}$
$B_s^0 \to \bar{D}^0\bar{K}^{*0}$	$(4.4 \pm 0.6) \times 10^{-4}$	$B^0 \to \bar{D}^0K^{*0}$	$(4.5 \pm 0.6) \times 10^{-5}$
$B^- \to D^0\rho^-$	$(9.39 \pm 0.21 \pm 0.50) \times 10^{-3}$	$B^+ \to \bar{D}^0K^{*+}$	$(5.3 \pm 0.4) \times 10^{-4}$

It should be noted that the matrix element of R_1^d vanishes in the massless limit of the down quark. As for R_4^d, the operator is related to other ones [43],

$$R_4^q = \frac{1}{4}\mathcal{O}_1^q + \frac{1}{2}\mathcal{O}_2^q + \frac{1}{2}\mathcal{O}_3^q - \frac{m_q}{m_b}\mathcal{O}_5^q + \frac{1}{2}R_2^q. \tag{B31}$$

Hence, $\langle \bar{B}_d|R_4^d|B_d\rangle$ can be represented by other matrix elements, which is used in our numerical result.

APPENDIX C: NUMERICAL INPUT

The experimental values of branching ratios for $B \to DM$ decays are extracted from the 2024 Particle Data Group publication [6] and given in Table I. The experimental values of the B-meson lifetimes from HFLAV [62] are given by

$$\begin{aligned}\tau(B^+) &= (1.638 \pm 0.004)\ \text{ps},\\ \tau(B_d) &= (1.519 \pm 0.004)\ \text{ps},\\ \tau(B_s) &= (1.520 \pm 0.005)\ \text{ps}.\end{aligned} \tag{C1}$$

Other input parameters necessary to implement the analysis are given in Table II.

TABLE II. Input parameters given in units of proper powers of GeV. For the parameters in $\Delta B = 0$ processes [47], m_b^{kin}, μ_π^2, and μ_G^2 are defined via the kinetic scheme [48,49] with the hard Wilsonian cutoff at 1 GeV. The bag parameters for dimension-six operators relevant to $\Delta B = 2$ processes [50] are based on the weighted average of the HQET sum rules and lattice QCD. For the form factors, the numerics in Table 4 of Ref. [16] are adopted, which are based on the recent phenomenological fit in Ref. [51] for the heavy-to-heavy form factors and on Refs. [52–54] for the heavy-to-light form factors.

$\alpha_s(M_Z)$	0.1180 ± 0.0009	[6]	M_W	80.3692 ± 0.0133	[6]
$\sin\theta_{12}$	0.22501 ± 0.00068	[6]	$\sin\theta_{13}$	$0.003732^{+0.000090}_{-0.000085}$	[6]
$\sin\theta_{23}$	$0.04183^{+0.00079}_{-0.00069}$	[6]	δ	1.147 ± 0.026	[6]
$\bar{m}_c(m_c)$	1.2730 ± 0.0046	[6]	$\bar{m}_b(m_b)$	4.183 ± 0.007	[6]
m_b^{kin}	4.573 ± 0.012	[47]	m_t^{pole}	172.4 ± 0.7	[6]
μ_π^2	0.477 ± 0.056	[47]	μ_G^2	0.306 ± 0.050	[47]
$\bar{B}_1(\bar{m}_b)$	$1.028^{+0.064}_{-0.056}$	[28]	$\bar{B}_2(\bar{m}_b)$	$0.988^{+0.087}_{-0.079}$	[28]
$\bar{\epsilon}_1(\bar{m}_b)$	$-0.107^{+0.028}_{-0.029}$	[28]	$\bar{\epsilon}_2(\bar{m}_b)$	-0.033 ± 0.021	[28]
$B_1^d(\bar{m}_b)$	0.835 ± 0.028	[50]	$B_2^d(\bar{m}_b)$	0.791 ± 0.034	[50]
$B_3^d(\bar{m}_b)$	0.775 ± 0.054	[50]	$B_4^d(\bar{m}_b)$	1.063 ± 0.041	[50]
$B_5^d(\bar{m}_b)$	0.994 ± 0.037	[50]	$B_{R_2}^s$	0.89 ± 0.38	[55]
$B_{R_3}^s$	1.07 ± 0.42	[55]	G_F	1.1663788×10^{-5}	[6]
$f_{\pi^\pm}$	0.1302 ± 0.0008	[56]	$f_{K^\pm}$	0.1557 ± 0.0003	[56]
f_D	0.2120 ± 0.0007	[56]	f_{D_s}	0.2499 ± 0.0005	[56]
f_B	0.1900 ± 0.0013	[56]	f_{B_s}	0.2303 ± 0.0013	[56]
f_ρ	0.213 ± 0.005	[52]	f_{K^*}	0.204 ± 0.007	[52]

(Table continued)

TABLE II. *(Continued)*

f_{D^*}	$0.242^{+0.020}_{-0.012}$	[57]	$f_{D_s^*}$	$0.293^{+0.019}_{-0.014}$	[57]
$F_0^{BD}(m_\pi^2)$	0.669 ± 0.010	[16]	$F_0^{BD}(m_K^2)$	0.672 ± 0.010	[16]
$A_0^{BD^*}(m_\pi^2)$	0.725 ± 0.014	[16]	$A_0^{BD^*}(m_K^2)$	0.732 ± 0.014	[16]
$F_+^{BD}(m_\rho^2)$	0.686 ± 0.010	[16]	$F_+^{BD}(m_{K^*}^2)$	0.692 ± 0.010	[16]
$F_0^{B_sK}(m_D^2)$	0.310	[16]	$F_0^{B\pi}(m_D^2)$	0.288	[16]
$F_+^{B_sK}(m_{D^*}^2)$	0.357	[16]	$F_+^{B\pi}(m_{D^*}^2)$	0.328	[16]
$A_0^{B_sK^*}(m_D^2)$	0.438	[16]	$A_0^{B\rho}(m_D^2)$	0.432	[16]
$\lvert V_{ud}\rvert$	0.97367 ± 0.00032	[6]	$\lvert V_{us}\rvert$	0.22431 ± 0.00085	[6]
$\lvert V_{cb}\rvert$	0.0397 ± 0.0006	[51]			

[1] M. Beneke, G. Buchalla, M. Neubert, and C. T. Sachrajda, QCD factorization for exclusive, nonleptonic B meson decays: General arguments and the case of heavy light final states, Nucl. Phys. **B591**, 313 (2000).

[2] C. W. Bauer, D. Pirjol, and I. W. Stewart, A proof of factorization for $B \to D\pi$, Phys. Rev. Lett. **87**, 201806 (2001).

[3] M. Bordone, N. Gubernari, T. Huber, M. Jung, and D. van Dyk, A puzzle in $\bar{B}^0_{(s)} \to D^{(*)+}_{(s)}\{\pi^-, K^-\}$ decays and extraction of the f_s/f_d fragmentation fraction, Eur. Phys. J. C **80**, 951 (2020).

[4] J. F. Krohn *et al.* (Belle Collaboration), Measurements of the branching fractions $\mathcal{B}(\bar{B}^0 \to D^{*+}\pi^-)$ and $\mathcal{B}(\bar{B}^0 \to D^{*+}K^-)$ and tests of QCD factorization, Phys. Rev. D **107**, 012003 (2023).

[5] J. Davies, S. Schacht, N. Skidmore, and A. Soni, Reappraisal of SU(3)-flavor breaking in B → DP, Phys. Rev. D **109**, 113006 (2024).

[6] S. Navas *et al.* (Particle Data Group Collaboration), Review of particle physics, Phys. Rev. D **110**, 030001 (2024).

[7] T. Huber, S. Kränkl, and X. Q. Li, Two-body non-leptonic heavy-to-heavy decays at NNLO in QCD factorization, J. High Energy Phys. 09 (2016) 112.

[8] M. L. Piscopo and A. V. Rusov, Non-factorisable effects in the decays $\bar{B}^0_s \to D^+_s\pi^-$ and $\bar{B}^0 \to D^+K^-$ from LCSR, J. High Energy Phys. 10 (2023) 180.

[9] B. Blok and I. E. Halperin, Regge asymptotics and color suppressed heavy meson decays, Phys. Lett. B **385**, 324 (1996).

[10] B. Blok, M. Gronau, and J. L. Rosner, Annihilation, rescattering, and CP asymmetries in B meson decays, Phys. Rev. Lett. **78**, 3999 (1997).

[11] J. F. Donoghue, E. Golowich, A. A. Petrov, and J. M. Soares, Systematics of soft final state interactions in B decay, Phys. Rev. Lett. **77**, 2178 (1996).

[12] C. K. Chua, W. S. Hou, and K. C. Yang, Final state rescattering and color suppressed $\bar{B}^0 \to D^{0(*)}h^0$ decays, Phys. Rev. D **65**, 096007 (2002).

[13] C. K. Chua and W. S. Hou, Implications of $\bar{B}^0 \to D^0\pi^0$ decays on $\bar{B} \to D\bar{K}, \bar{D}\,\bar{K}$ decays, Phys. Rev. D **72**, 036002 (2005).

[14] C. K. Chua and W. S. Hou, Rescattering effects in $\bar{B}_{u,d,s} \to DP, \bar{D}P$ decays, Phys. Rev. D **77**, 116001 (2008).

[15] C. K. Chua, Revisiting final state interaction in charmless $B_q \to PP$ decays, Phys. Rev. D **97**, 093004 (2018).

[16] M. Endo, S. Iguro, and S. Mishima, Revisiting rescattering contributions to $\bar{B}_{(s)} \to D^{(*)}_{(s)}M$ decays, J. High Energy Phys. 01 (2022) 147.

[17] F. M. Cai, W. J. Deng, X. Q. Li, and Y. D. Yang, Probing new physics in class-I B-meson decays into heavy-light final states, J. High Energy Phys. 10 (2021) 235.

[18] S. Iguro and T. Kitahara, Implications for new physics from a novel puzzle in $\bar{B}^0_{(s)} \to D^{(*)+}_{(s)}\{\pi^-, K^-\}$ decays, Phys. Rev. D **102**, 071701 (2020).

[19] R. Fleischer and E. Malami, Using $B^0_s \to D^\mp_s K^\pm$ decays as a portal to new physics, Phys. Rev. D **106**, 056004 (2022).

[20] R. Fleischer and E. Malami, Revealing new physics in $\bar{B}^0_s \to D^\mp_s K^\pm$ decays, Eur. Phys. J. C **83**, 420 (2023).

[21] T. Gershon, A. Lenz, A. V. Rusov, and N. Skidmore, Testing the standard model with CP asymmetries in flavor-specific nonleptonic decays, Phys. Rev. D **105**, 115023 (2022).

[22] A. Lenz, J. Müller, M. L. Piscopo, and A. V. Rusov, Taming new physics in $b \to c\bar{u}d(s)$ with $\tau(B^+)/\tau(B_d)$ and a^d_{sl}, J. High Energy Phys. 09 (2023) 028.

[23] A. Lenz, M. L. Piscopo, and A. V. Rusov, Disintegration of beauty: A precision study, J. High Energy Phys. 01 (2023) 004.

[24] A. Lenz and G. Tetlalmatzi-Xolocotzi, Model-independent bounds on new physics effects in non-leptonic tree-level decays of B-mesons, J. High Energy Phys. 07 (2020) 177.

[25] G. Buchalla, A. J. Buras, and M. E. Lautenbacher, Weak decays beyond leading logarithms, Rev. Mod. Phys. **68**, 1125 (1996).

[26] M. Egner, M. Fael, A. Lenz, M. L. Piscopo, A. V. Rusov, K. Schönwald, and M. Steinhauser, Total decay rates of B mesons at NNLO-QCD, arXiv:2412.14035.

[27] A. Lenz, Lifetimes and heavy quark expansion, Int. J. Mod. Phys. A **30**, 1543005 (2015).

[28] M. Kirk, A. Lenz, and T. Rauh, Dimension-six matrix elements for meson mixing and lifetimes from sum rules, J. High Energy Phys. 12 (2017) 068; 06 (2020) 162(E).

[29] H. Y. Cheng, Phenomenological study of heavy hadron lifetimes, J. High Energy Phys. 11 (2018) 014.

[30] E. Golowich, S. Pakvasa, and A. A. Petrov, New physics contributions to the lifetime difference in $D^0 - \overline{D^0}$ mixing, Phys. Rev. Lett. **98**, 181801 (2007).

[31] C. Bobeth and U. Haisch, New physics in Γ_{12}^s: $(\bar{s}b)(\bar{\tau}\tau)$ operators, Acta Phys. Pol. B **44**, 127 (2013).

[32] A. Badin, F. Gabbiani, and A. A. Petrov, Lifetime difference in B_s mixing: Standard model and beyond, Phys. Lett. B **653**, 230 (2007).

[33] B. A. Dobrescu, P. J. Fox, and A. Martin, *CP* violation in B_s mixing from heavy Higgs exchange, Phys. Rev. Lett. **105**, 041801 (2010).

[34] Y. Bai and A. E. Nelson, *CP* violating contribution to $\Delta\Gamma$ in the B_s system from mixing with a hidden pseudoscalar, Phys. Rev. D **82**, 114027 (2010).

[35] J. Kubo and A. Lenz, Large loop effects of extra SUSY Higgs doublets to *CP* violation in B^0 mixing, Phys. Rev. D **82**, 075001 (2010).

[36] S. Oh and J. Tandean, Anomalous *CP*-violation in $B_s - \bar{B}_s$ mixing due to a light spin-one particle, Phys. Lett. B **697**, 41 (2011).

[37] M. Trott and M. B. Wise, On theories of enhanced *CP* violation in $B_{s,d}$ meson mixing, J. High Energy Phys. 11 (2010) 157.

[38] J. E. Kim, M. S. Seo, and S. Shin, The D0 same-charge dimuon asymmetry and possibile new *CP* violation sources in the $B_s - \bar{B}_s$ system, Phys. Rev. D **83**, 036003 (2011).

[39] W. Altmannshofer, M. Carena, S. Gori, and A. de la Puente, Signals of *CP* violation beyond the MSSM in Higgs and flavor physics, Phys. Rev. D **84**, 095027 (2011).

[40] S. Nandi and D. London, $B_s^0(\bar{B}_s^0) \to D_{CP}^0 K\bar{K}$: Detecting and discriminating new physics in $B_s^0 - \bar{B}_s^0$ mixing, Phys. Rev. D **85**, 114015 (2012).

[41] T. Inami and C. S. Lim, Effects of superheavy quarks and leptons in low-energy weak processes $K_L \to \mu\bar{\mu}$, $K^+ \to \pi^+\nu\bar{\nu}$ and $K^0 \leftrightarrow \overline{K^0}$, Prog. Theor. Phys. **65**, 297 (1981); **65**, 1772(E) (1981).

[42] M. Beneke, G. Buchalla, and I. Dunietz, Width difference in the $B_s - \overline{B_s}$ system, Phys. Rev. D **54**, 4419 (1996); **83**, 119902(E) (2011).

[43] M. Ciuchini, E. Franco, V. Lubicz, F. Mescia, and C. Tarantino, Lifetime differences and *CP* violation parameters of neutral B mesons at the next-to-leading order in QCD, J. High Energy Phys. 08 (2003) 031.

[44] M. Beneke, G. Buchalla, C. Greub, A. Lenz, and U. Nierste, Next-to-leading order QCD corrections to the lifetime difference of B_s mesons, Phys. Lett. B **459**, 631 (1999).

[45] M. Beneke, G. Buchalla, A. Lenz, and U. Nierste, *CP* asymmetry in flavor specific B decays beyond leading logarithms, Phys. Lett. B **576**, 173 (2003).

[46] I. Adachi *et al.* (Belle-II Collaboration), Measurement of the branching fraction of the decay $B^- \to D^0\rho(770)^-$ at Belle II, Phys. Rev. D **109**, L111103 (2024).

[47] M. Bordone, B. Capdevila, and P. Gambino, Three loop calculations and inclusive V_{cb}, Phys. Lett. B **822**, 136679 (2021).

[48] I. I. Y. Bigi, M. A. Shifman, N. G. Uraltsev, and A. I. Vainshtein, Sum rules for heavy flavor transitions in the SV limit, Phys. Rev. D **52**, 196 (1995).

[49] I. I. Y. Bigi, M. A. Shifman, N. Uraltsev, and A. I. Vainshtein, High power n of m_b in beauty widths and $n = 5 \to \infty$ limit, Phys. Rev. D **56**, 4017 (1997).

[50] L. Di Luzio, M. Kirk, A. Lenz, and T. Rauh, ΔM_s theory precision confronts flavour anomalies, J. High Energy Phys. 12 (2019) 009.

[51] S. Iguro and R. Watanabe, Bayesian fit analysis to full distribution data of $\overline{B} \to D^{(*)}\ell\bar{\nu}$: $|V_{cb}|$ determination and new physics constraints, J. High Energy Phys. 08 (2020) 006.

[52] A. Bharucha, D. M. Straub, and R. Zwicky, $B \to V\ell^+\ell^-$ in the standard model from light-cone sum rules, J. High Energy Phys. 08 (2016) 098.

[53] P. Ball and R. Zwicky, New results on $B \to \pi, K, \eta$ decay formfactors from light-cone sum rules, Phys. Rev. D **71**, 014015 (2005).

[54] A. Khodjamirian and A. V. Rusov, $B_s \to K\ell\nu_\ell$ and $B_{(s)} \to \pi(K)\ell^+\ell^-$ decays at large recoil and CKM matrix elements, J. High Energy Phys. 08 (2017) 112.

[55] C. T. H. Davies, J. Harrison, G. Peter Lepage, C. J. Monahan, J. Shigemitsu, and M. Wingate (HPQCD Collaboration), Lattice QCD matrix elements for the $B_s^0 - \bar{B}_s^0$ width difference beyond leading order, Phys. Rev. Lett. **124**, 082001 (2020).

[56] Y. Aoki *et al.* (Flavour Lattice Averaging Group (FLAG) Collaboration), FLAG review 2021, Eur. Phys. J. C **82**, 869 (2022).

[57] P. Gelhausen, A. Khodjamirian, A. A. Pivovarov, and D. Rosenthal, Decay constants of heavy-light vector mesons from QCD sum rules, Phys. Rev. D **88**, 014015 (2013); **89**, 099901(E) (2014); **91**, 099901(E) (2015).

[58] K. G. Chetyrkin, J. H. Kuhn, and M. Steinhauser, RunDec: A *Mathematica* package for running and decoupling of the strong coupling and quark masses, Comput. Phys. Commun. **133**, 43 (2000).

[59] A. Lenz and U. Nierste, Theoretical update of $B_s - \bar{B}_s$ mixing, J. High Energy Phys. 06 (2007) 072.

[60] M. Artuso, G. Borissov, and A. Lenz, *CP* violation in the B_s^0 system, Rev. Mod. Phys. **88**, 045002 (2016).

[61] J. Albrecht, F. Bernlochner, A. Lenz, and A. Rusov, Lifetimes of b-hadrons and mixing of neutral B-mesons: Theoretical and experimental status, Eur. Phys. J. Special Topics **233**, 359 (2024).

[62] Y. S. Amhis *et al.* (HFLAV Collaboration), Averages of b-hadron, c-hadron, and τ-lepton properties as of 2021, Phys. Rev. D **107**, 052008 (2023).

[63] R. Aaij *et al.* (LHCb Collaboration), Physics case for an LHCb upgrade II—Opportunities in flavour physics, and beyond, in the HL-LHC era, arXiv:1808.08865.

[64] A. Cerri, V. V. Gligorov, S. Malvezzi, J. Martin Camalich, J. Zupan, S. Akar, J. Alimena, B. C. Allanach, W. Altmannshofer, L. Anderlini *et al.*, Report from working group 4: Opportunities in flavour physics at the HL-LHC and HE-LHC, CERN Yellow Rep. Monogr. **7**, 867 (2019).

[65] M. Neubert, Heavy quark symmetry, Phys. Rep. **245**, 259 (1994).